BEST AVAILABLE IMAGES

Defective images within this document are accurate representations of the original documents submitted by the applicant.

Defects in the images may include (but are not limited to):

- BLACK BORDERS
- TEXT CUT OFF AT TOP, BOTTOM OR SIDES
- FADED TEXT
- ILLEGIBLE TEXT
- SKEWED/SLANTED IMAGES
- COLORED PHOTOS
- BLACK OR VERY BLACK AND WHITE DARK PHOTOS
- GRAY SCALE DOCUMENTS

IMAGES ARE BEST AVAILABLE COPY.

As rescanning documents *will not* correct images, please do not report the images to the Image Problem Mailbox.

REMARKS

By the present amendment, the preamble of all claims has been amended to recite a non-human mammalian model animal. Further, new claims 9-18 have been added. Support for the new claims is found in the original application, in particular on page 21, lines 7-9 (claims 9-12), page 4, lines 1-8, page 22, lines 17-19, page 24, lines 5-6, and page 25, lines 15-18 (claims 13-15), page 11, lines 20-23 (claims 16-17), and page 3, lines 21-24 (claim 18).

Also, the specification has been amended to introduce SEQ ID NOs on page 17. A sequence listing in disk and paper form is being submitted with this paper.

Claims 1-18 are pending in the present application. The claims are directed to a non-human mammalian model animal for psychiatric disorders. Claim 1 is the only independent claim.

As a preliminary, in the Office Action, it is indicated that, although priority of Japanese application No. JP 2000-118288 filed on April 19, 2000 is claimed, no official copy of the priority document was filed.

Applicants submit that the priority document was filed in parent application Serial No. 09/835,627, as indicated in the application filing transmittal of the present application. Thus, acknowledgment of receipt of the official copy of the priority document is respectfully requested.

Next, in the Office Action, the application is objected to for lack of compliance with sequence listing disclosure rules.

A Submission of Sequence Listing is submitted with this paper. The specification has been amended accordingly to introduce sequence listing numbers. Accordingly, withdrawal of the objection is respectfully requested.

Next, in the Office Action, claims 1-8 are rejected under 35 U.S.C. 101 as directed to non-patentable subject matter, on the ground that the term "mammalian" does not exclude humans.

The preamble of all claims has been amended to recite "non-human mammalian" as suggested in the Office Action. Accordingly, it is submitted that the rejection should be withdrawn.

Next, in the Office Action, claims 1-8 are rejected under 35 U.S.C. 112, first paragraph, as not enabled. It is alleged in the Office Action that the specification is not enabling for the following subject matter:

1. A mammal other than mice, on the grounds that ES cells for other than mice were not available at the time of the invention, and that targeted insertion using the two other methods mentioned in the specification (genomic DNA insertion in pronuclear embryonic phase and retrovirus infection of early phase embryo) are highly unpredictable.
2. A non-homozygous animal, on the ground that the phenotype resulting from mutation of heterozygous animals is unpredictable.
3. A deficiency of function other than complete shutting off of the PACAP gene.
4. A mouse not having the phenotype described in the specification.

The rejection is respectfully traversed. With respect to point 1 above, it is submitted that, not only ES cell technology, but also other technologies, as discussed in the present specification, for example on pages 7-8. Further, other technologies such as RNAi (RNA interference) or random integration have become widely available. These technologies are known to a person of the art to be applicable to mice as well as other mammals, and even Drosophila or nematodes such as *C. elegans*. Accordingly, a person of ordinary skill in the art would have been able to select an

appropriate technology, among the technologies available at the effective filing date of the application, to obtain the model mammalian animal of the present claims without undue experimentation.

In addition, this objection is also respectfully traversed as it applies to dependent claims 7-8, which recite a rodent, and a mice, respectively.

Regarding point 2 above, the position set forth in the Office Action is respectfully traversed. Reference is made to the Examples in the present specification, which discuss heterozygous disruption of the PACAP gene. For example, it is explained on page 21, lines 15-18 that heterozygous mice showed a reduction in expression of the mature peptide while homozygous mice showed a complete disappearance of expression. Also, the behavior of heterozygous mice is evaluated (see page 23, lines 7-9, or the Table on page 35, for example). In summary, a person of ordinary skill in the art would clearly understand from the original application (i) that the present invention can be successfully performed to obtain a heterozygous model animal, and (ii) that the heterozygous model animal can be used for its purpose as a model for psychiatric disorders.

In addition, it is submitted that the objection does not apply to present claim 10, which recites a homozygous chromosome of a somatic cell and a germ cell with deficiency of function of pituitary adenylate cyclase-activating polypeptide gene.

Regarding point 3 above, the position set forth in the Office Action is also respectfully traversed. The Examples of the original application, which are discussed above with respect to point 2, teach that a partial shut off of the PACAP gene (i) is practicable by a person of ordinary skill in the art, and (ii) provides results that can be used by that person.

Further, reference is made to the attached publication Neuroreport 2003, Nov. 14, 14(16),

2095-98, which demonstrates successful application of PACAP deficiency to heterozygous animals.

In addition, it is submitted that the objection does not apply to present claim 12, which recites that expression of a mature peptide coding sequence of the gene has disappeared.

Finally, regarding point 4 above, it is submitted that it would be clearly apparent that the PACAP gene-deficient animals are useful for studying the in vivo function of PACAP-dependent signaling, as described for example on page 3, lines 16-19 of the present specification. The link between PACAP deficiency and psychiatric behavior is already studied by a person of ordinary skill in the art as discussed in the introduction to the present specification. Therefore, a person of ordinary skill in the art would be able to practice the presently claimed invention with regard to a variety of specific symptoms.

In particular, reference is made to the three attached publications Brain Res. 874, 194-199 (2000), J. Neurosci. 21, 5520-5527 (2001), Biochem. Biophys. Res. Comm. 297, 427-432 (2002), and Zan et al., Nature Biotechnology, published online doi:10.1038/nbt830 (2003), which show that PACAP deficiencies was conventionally related to psychiatric disorders.

Further, with respect to heterozygous animal, it is submitted that this animal is useful for preparing a homozygous animal, as discussed in particular in the Examples of the present specification.

In addition, it is submitted that this objection does not apply to present claims 13-18 which recite a phenotype and/or useful characteristics of the animal.

In view of the above, it is submitted that the rejection should be withdrawn.

In conclusion, the invention as presently claimed is patentable. It is believed that the claims are in allowable condition and a notice to that effect is earnestly requested.

In the event there is, in the Examiner's opinion, any outstanding issue and such issue may be resolved by means of a telephone interview, the Examiner is respectfully requested to contact the undersigned attorney at the telephone number listed below.

In the event this paper is not considered to be timely filed, the Applicants hereby petition for an appropriate extension of the response period. Please charge the fee for such extension and any other fees which may be required to our Deposit Account No. 50-2866.

Respectfully submitted,

WESTERMAN, HATTORI, DANIELS & ADRIAN, LLP

Nicolas E. Seckel
Attorney for Applicants
Reg. No. 44,373

Atty. Docket No.: 010541A
Customer No.: 38834
1250 Connecticut Avenue NW Suite 700
Washington, D.C. 20036
Tel: (202) 822-1100
Fax: (202) 822-1111
NES:rep
Attachments: 5 References

Impaired long-term potentiation *in vivo* in the dentate gyrus of pituitary adenylate cyclase-activating polypeptide (PACAP) or PACAP type I receptor-mutant mice

Shogo Matsuyama,[CA] Akira Matsumoto,[1] Hitoshi Hashimoto,[2] Norihito Shintani[2] and Akemichi Baba[2,3]

Division of Molecular Pharmacology and Pharmacogenomics, Department of Genome Sciences, Kobe University Graduate School of Medicine, 7-5-1 Kusunoki-cho, Chuo-ku, Kobe 650-0017; [1]Brain Disease Pathogenesis Research Division, Foundation for Biomedical Research and Innovation, Kobe, 650-0047; [2]Laboratory of Molecular Neuropharmacology, Graduate School of Pharmaceutical Sciences; [3]Laboratory of Molecular Pharmacology, Graduate School of Medicine, Osaka University, Suita, Osaka 565-0871, Japan

[CA]Corresponding Author: shogo@med.kobe-u.ac.jp

Received 9 May 2003; accepted 11 June 2003

DOI: 10.1097/01.wnr.0000090953.15465.5a

The present study was conducted to clarify a role of pituitary adenylate cyclase-activating polypeptide (PACAP) and PACAP type I receptor (PAC_1R) in learning and memory function. We demonstrated long-term potentiation (LTP) *in vivo* in the dentate gyrus of PAC_1R exon 2-deficient ($PAC_1R^{-/-}$) mice and heterozygous PACAP-deficient ($PACAP^{+/-}$) mice using extracellular recording techniques. We used two paradigms of tetanic stimulation, suprathreshold and at threshold tetanus, which both induced LTP *in vivo* in $PAC_1R^{-/-}$ and $PACAP^{+/-}$ mice. However, the population spike of 'at threshold' but not 'suprathreshold' LTP decreased significantly in $PAC_1R^{-/-}$ and $PACAP^{+/-}$ mice. At threshold LTP of $PACAP^{+/-}$ mice was impaired greater than the one of $PAC_1R^{-/-}$ mice. Thus, both PACAP and PAC_1R could contribute to the establishment of LTP in a gene dosage-dependent manner, although PACAP rather than PAC_1R might play a pivotal role in learning and memory function. *NeuroReport* 14:2095–2098 © 2003 Lippincott Williams & Wilkins.

Key words: Hippocampus; *In vivo*; Long-term potentiation; Mouse; Pituitary adenylate cyclase-activating polypeptide; Pituitary adenylate cyclase-activating polypeptide type I receptor

INTRODUCTION

Pituitary adenylate cyclase-activating polypeptide (PACAP) belongs to the vasoactive intestinal peptide (VIP)/secretin/glucagon family and exists in two α-amidated forms, PACAP38 and PACAP27 [1,2]. PACAP is distributed in central and peripheral nervous systems and may function as neurotransmitter and/or neuromodulator [2]. PACAP binds to PACAP-preferring type 1 (PAC_1) and VIP-shared type 2 ($VPAC_1$ and $VPAC_2$) receptors. PAC_1R is predominantly expressed in the CNS and implicates in neurotransmission, neurotrophic actions and synaptic plasticity [1]. Especially the neocortex, the limbic system, and brain stem exhibit a strong expression of PAC_1R mRNA [3].

Drosophila harboring a mutation in the PACAP-related gene *amnesiac* display deficits in associative learning [4,5]. PACAP and PAC_1R are involved in improving learning and memory function in animal behavioral experiments [6,7]. Long-term potentiation (LTP) is a long-lasting increase in the efficacy of synaptic transmission [8] and is assumed to underlie plastic changes associated with learning and memory [9,10]. Recently, PACAP and PAC_1R have been reported to play a role in the establishment of LTP *in vitro* in the hippocampal slice preparations [6,11,12]. However, the functions of PACAP and PAC_1R in LTP *in vivo* in the hippocampal formations are unknown, and there has been no report about LTP *in vivo* in PACAP or PAC_1R mutant mice. Moreover, the intact preparation for LTP experiments is especially relevant because all of the normal connections of the hippocampal formation are preserved, linking with the animal behavioral studies. We showed the difference of LTP phenotype produced by two paradigms of tetanic stimulation, suprathreshold and at threshold, in the intact mouse dentate gyrus, and proposed that at threshold tetanus which is insufficient to activate the LTP-expressing mechanism fully can express LTP similar to suprathreshold LTP under physiologically relevant conditions [13]. We generated heterozygous PACAP-deficient ($PACAP^{+/-}$) mice and PAC_1R exon 2-deficient ($PAC_1R^{-/-}$) mice: PACAP38 expression in the brain of $PACAP^{+/-}$ mice is one third of wild-type mice [15] and $PAC_1R^{-/-}$ mice have about

25% of ^{125}I-PACAP27 binding density but not a null mutation of PAC_1R in their brain [14]. Taken together, we speculate that PACAP or PAC_1R mutant mice might show impaired LTP *in vivo*.

Here, we aim to elucidate the role of PACAP and PAC_1R in learning and memory function by investigating LTP *in vivo* in the dentate gyrus of $PACAP^{+/-}$ mice and $PAC_1R^{-/-}$ mice using two paradigms of tetanus.

MATERIALS AND METHODS

Subjects: Mice lacking PAC_1 receptor exon 2 were generated using 129/Sv mouse-derived D3 embryonic stem (ES) cells as described previously [14]. PAC_1 receptor mutant mice were backcrossed for ≥ 10 generations onto a C57BL/6J mouse background and used in this study. Mice lacking PACAP were generated using 129/Ola mouse-derived E14tg2a ES cells (clone EB3) as described previously [16]. The mutant mice were backcrossed for six generations onto a C57BL/6J mouse background and used in this study. Adult mice 2–3 months old were maintained at 21–24°C on a 12:12 h light:dark schedule (lights on at 08:00 h) with free access to water and rodent chow.

LTP recording in in vivo *mouse dentate gyrus:* Experiments were performed on mice *in vivo* prepared as described previously [16]. Animal care and handling were done strictly in accordance with the Guidelines for Animal Experimentation at Kobe University Graduate School of Medicine. Briefly, mice were anesthetized with urethane (1.2 g/kg, i.p. followed by supplemental injections of 0.2–0.6 g/kg as needed) and placed in the stereotaxic apparatus. Body temperature was maintained at 37°C using a heated mat (BRC, Nagoya, Japan). A glass recording electrode with 9–12 μm tip diameter, back-filled with 0.9% NaCl, was lowered to the cell body layer of dentate granule cells. Initial responses were obtained using a cathodal stimulation (6.0–8.0 V, 0.1 Hz, 0.1 ms duration) of the perforant path. After electrode insertion and population responses were obtained, the preparation was allowed to stabilize for 90 min prior to baseline recording. Voltage was reduced so that baseline spike amplitude was one-third the maximum asymptotic value. The LTP-inducing voltage used was the lowest voltage level that could evoke a maximum asymptotic spike amplitude. We used two paradigms of stimulation, suprathreshold and at threshold to induce LTP [13]. Suprathreshold LTP consisted of three trains with an inter-train interval of 10 s with each train consisting of eight 0.4 ms 400 Hz pulses. At threshold LTP consisted of one train of stimulation. We plotted only the population spike without the EPSP slope because the potentiated change in population spikes is similar to that of the EPSP slope during LTP in this procedure [16]. At 5 min intervals, the population spikes induced by five successive stimulations were averaged and analyzed with a personal computer (PowerLab System, BRC, Nagoya, Japan). Data are expressed as mean ± s.e.m. from (n). Statistical analysis was performed using the unpaired t-test between wild-type and mutant mice 120 min after tetanic stimulation. Differences at $p < 0.05$ were considered statistically significant.

RESULTS

Impaired LTP in vivo expressed by at threshold but not suprathreshold tetanus in the dentate gyrus of $PAC_1R^{-/-}$ mice: We applied two paradigms of tetanus into $PAC_1R^{-/-}$ mice which we had generated [14]. When induced by tetanus, the potentiated response was maintained throughout the 120 min recording. The population spike of at threshold but not suprathreshold LTP decreased in $PAC_1R^{-/-}$ mice (Fig. 1). Figure 1a shows representative traces at the

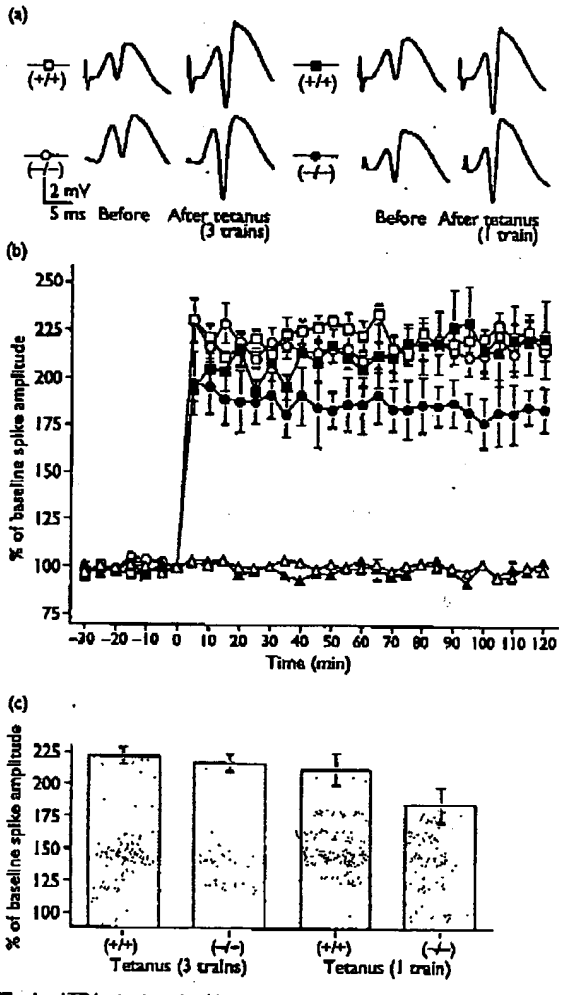

Fig. 1. LTP *in vivo* impaired by at threshold but not suprathreshold tetanus in the dentate gyrus of $PAC_1R^{-/-}$ mice. (a) Representative traces are recorded from the granule cell layer before and after tetanus in $PAC_1R^{+/+}$ and $PAC_1R^{-/-}$ mice. (b) The time course of $PAC_1R^{+/+}$ and $PAC_1R^{-/-}$ mice, $n = 5$ for each group, is shown for 120 min after tetanus. Control of $PAC_1R^{+/+}$ mice (open triangles) and $PAC_1R^{-/-}$ mice (closed triangles). Three trains of tetanus were applied at 0 min in $PAC_1R^{+/+}$ mice (open squares) and $PAC_1R^{-/-}$ mice (open circles). One train of tetanus was applied at 0 min in $PAC_1R^{+/+}$ mice (closed squares) and $PAC_1R^{-/-}$ mice (closed circles). Each point represents the mean (± s.e.m.) percentage of basal population spike amplitude at 0 min. (c) The population spike of LTP is shown as the mean ± s.e.m. for 2 h after tetanus (1 and 3 trains) in $PAC_1R^{+/+}$ and $PAC_1R^{-/-}$ mice.

indicated conditions. Percent of baseline spike amplitude for 120 min recording after suprathreshold LTP induction was 217.8 ± 6.8 for PAC$_1$R$^{-/-}$ mice and 222.9 ± 6.6 for PAC$_1$R$^{+/+}$ mice (Fig. 1c). Percent of baseline spike amplitude for 120 min recording after at threshold LTP induction was 186.8 ± 13.8 for PAC$_1$R$^{-/-}$ mice and 213.1 ± 12.0 for PAC$_1$R$^{+/+}$ mice (Fig. 1c). A significant difference of the population spike 120 min after at threshold tetanus was found between PAC$_1$R$^{-/-}$ and PAC$_1$R$^{+/+}$ mice (183.5 ± 11.6% for PAC$_1$R$^{-/-}$ mice and 217.9 ± 14.7% for PAC$_1$R$^{+/+}$ mice; $p < 0.05$, $n = 5$ for each group). There was no significant difference of the population spike 120 min after suprathreshold tetanus between PAC$_1$R$^{-/-}$ and PAC$_1$R$^{+/+}$ mice (216.0 ± 4.8% for PAC$_1$R$^{-/-}$ mice and 220.6 ± 6.4% for PAC$_1$R$^{+/+}$ mice; $p > 0.05$, $n = 5$ for each group).

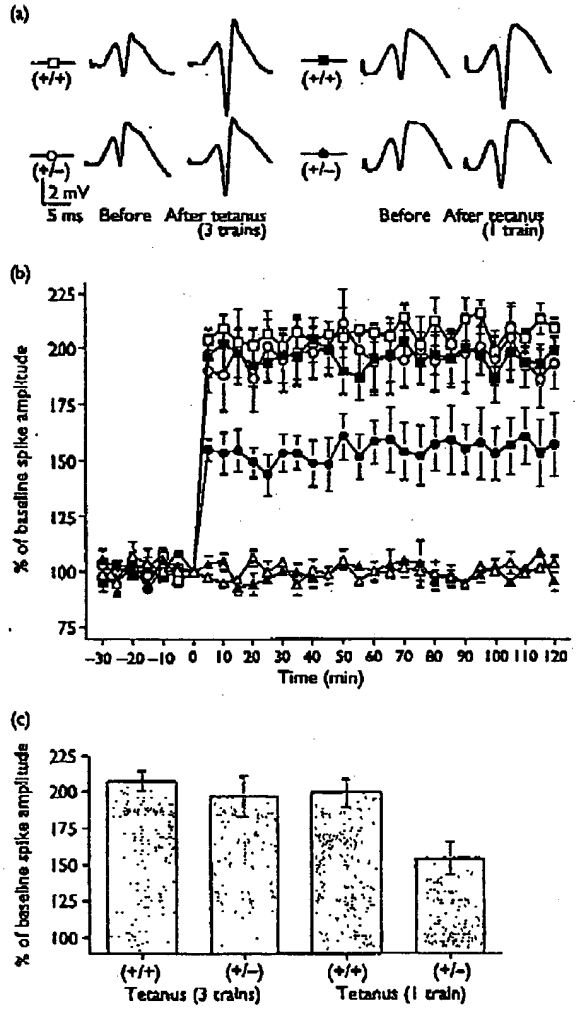

Fig. 2. LTP *in vivo* impaired by at threshold but not suprathreshold tetanus in the dentate gyrus of PACAP$^{+/-}$ mice. (a) Representative traces are recorded from the granule cell layer before and after tetanus in PACAP$^{+/+}$ and PACAP$^{+/-}$ mice. (b) The time course of PACAP$^{+/+}$ and PACAP$^{+/-}$ mice, $n = 5$ for each group. Is shown for 120 min after tetanus. Control of PACAP$^{+/+}$ mice (open triangles) and PACAP$^{+/-}$ mice (closed triangles). Three trains of tetanus were applied at 0 min in PACAP$^{+/+}$ mice (open squares) and PACAP$^{+/-}$ mice (open circles). One train of tetanus was applied at 0 min in PACAP$^{+/+}$ mice (closed squares) and PACAP$^{+/-}$ mice (closed circles). Each point represents the mean ± s.e.m. percentage of basal population spike amplitude at 0 min. (c) The population spike of LTP is shown as the mean ± s.e.m. for 2 h after tetanus (1 and 3 trains) in PACAP$^{+/+}$ and PACAP$^{+/-}$ mice.

Impaired LTP* in vivo *expressed by at threshold but not suprathreshold tetanus in the dentate gyrus of PACAP$^{+/-}$ mice: We applied two paradigms of tetanus into PACAP$^{+/-}$ mice which we had generated [15]. When induced by tetanus, the potentiated response was maintained throughout the 120 min recording. The population spike of at threshold but not suprathreshold LTP decreased in PACAP$^{+/-}$ mice (Fig. 2). Figure 2a shows representative traces at the indicated conditions. Percent of baseline spike amplitude for 120 min recording after suprathreshold LTP induction was 197.2 ± 13.5 for PACAP$^{+/-}$ mice and 207.3 ± 6.7 for PACAP$^{+/+}$ mice (Fig. 2c). Percent of baseline spike amplitude for 120 min recording after at threshold LTP induction was 155.6 ± 11.2 for PACAP$^{+/-}$ mice and 199.8 ± 9.4 for PACAP$^{+/+}$ mice (Fig. 2c). A significant difference of the population spike 120 min after at threshold tetanus was found between PACAP$^{+/-}$ mice and PACAP$^{+/+}$ mice (157.5 ± 14.3% for PACAP$^{+/-}$ mice and 203.6 ± 7.3% for PACAP$^{+/+}$ mice; $p < 0.05$, $n = 5$ for each group). There was no significant difference of the population spike 120 min after suprathreshold tetanus between PACAP$^{+/-}$ mice and PACAP$^{+/+}$ mice (192.5 ± 12.5% for PACAP$^{+/-}$ mice and 205.8 ± 4.3% for PACAP$^{+/+}$ mice; $p > 0.05$, $n = 5$ for each group).

DISCUSSION

For the first time, the present study demonstrates LTP *in vivo* in the dentate gyrus of PACAP-mutant (PACAP$^{+/-}$) mice and PAC$_1$R-deficient (PAC$_1$R$^{-/-}$) mice. PACAP and PAC$_1$R are widely distributed in the brain and involved in the regulation of many neurotransmitters and neuropeptides: in the hippocampal formation, PACAP-containing neurons and PAC$_1$R were abundant [2]. The hippocampal formation, which is a center for learning and memory, receives many neural projections from other regions of the brain [17]. These findings imply that learning and memory could be affected by PACAP and PAC$_1$R present on not only hippocampus but also other regions. Thus, it is important and indispensable to investigate LTP by *in vivo* procedure to understand the role of PACAP and PAC$_1$R on learning and memory function more precisely. The PACAP$^{-/-}$ mice are born in the expected Mendelian ratios, but have a high early mortality rate and ~50% of the PACAP$^{-/-}$ pups die of unknown causes before weaning [15]. The surviving PACAP$^{-/-}$ females exhibit reduced fertility, which is partly due to reduced mating frequency, and show inadequate maternal behaviors [18]. Gray *et al.* [19] also reported that targeted deletion of PACAP is associated with an extremely high mortality rate. Thus, we can not help using PACAP$^{+/-}$ mice in this study because of being impossible to maintain the number of PACAP$^{-/-}$ mice necessary for LTP *in vivo* experiments.

PAC_1R is localized in the granule cells of the dentate gyrus [20,21], suggesting the involvement of PAC_1R in LTP in the dentate gyrus. Indeed, our findings showed that at threshold but not suprathreshold LTP *in vivo* was significantly impaired in the dentate gyrus of $PAC_1R^{-/-}$ mice (Fig. 1). In view of the two paradigms of tetanic stimulation, at threshold LTP might be impaired under physiologically irrelevant conditions like mutant mice, whereas suprathreshold LTP in which the LTP-expressing mechanism is activated fully might be not changed. Moreover, one possible explanation for this result is that $PAC_1R^{-/-}$ mice have about 25% of ^{125}I-PACAP27 binding density in the brain [14], leading to a gene dosage effect of the mutations in the PAC_1R locus on LTP, and the other is that $VPAC_1R$ and/or $VPAC_2R$ might compensate for PAC_1R as they are present in the dentate gyrus, through which PACAP stimulates cyclic AMP production with a potency similar to that for PAC_1R [2]. Otto *et al.* [6] showed that $VPAC_1R$ and $VPAC_2R$ were not up-regulated in $PAC_1R^{-/-}$ mice. The finding that LTP *in vitro* was not impaired in the dentate gyrus of hippocampal slice preparations of $PAC_1R^{-/-}$ mice [6] was consistent with suprathreshold LTP *in vivo* in $PAC_1R^{-/-}$ mice (Fig. 1). Interestingly, $PAC_1R^{-/-}$ mice showed just a mild deficit in performing on memory tasks [22] and a selective deficit in a hippocampus-dependent associative learning paradigm [6], supporting our LTP *in vivo* findings. Taken together, the role of PAC_1R in LTP is subtle and it is suggested that PAC_1R only plays a limited role in learning and memory.

There have been no reports about hippocampal LTP *in vitro* and *in vivo* in PACAP-mutant mice. However, a high concentration (1 μM) of PACAP38 induced a long-lasting facilitation similar to LTP in the dentate gyrus of the hippocampal slice preparations [11] and PACAP38 expression in the brain of $PACAP^{+/-}$ mice was one-third of $PACAP^{+/+}$ mice [15], leading to the possibility that the decreased expression of PACAP in neurons of $PACAP^{+/-}$ mice contributes to impaired LTP in the dentate gyrus. Indeed, at threshold but not suprathreshold LTP *in vivo* was significantly impaired in the dentate gyrus of $PACAP^{+/-}$ mice (Fig. 2). One possible explanation is that a sufficient amount of PACAP is released by suprathreshold but not at threshold tetanus of the perforant path in $PACAP^{+/-}$ mice, supported by the existence of PACAP containing neurons in the entorhinal cortex projecting to the dentate granule cells via the perforant path [23]. It remains to clarify another possibility that the decreased PACAP in postsynaptic granule cells might be involved in the induction and maintenance of LTP, as the granule cells in the dentate gyrus contain large amount of PACAP [23]. Moreover, at threshold LTP $PACAP^{+/-}$ mice were impaired more than $PAC_1R^{-/-}$ mice (Fig. 1, Fig. 2), suggesting that a contribution of PACAP to LTP is greater than that of PAC_1R. PACAP38 improved the learning and memory processes in a passive avoidance paradigm by dopaminergic, adrenergic, and serotonergic mediation [7]. PACAP increased cholinergic activity at the level of the septohippocampal projection, which plays an important role in learning and memory [24]. Taken together, it is suggested that PACAP play a critical role in learning and memory in cooperation with other mediators (e.g. neurotransmitters).

In conclusion, PACAP rather than PAC_1R play a pivotal role in learning and memory function although both PACAP and PAC_1R contribute to LTP. Interestingly, a gene dosage effect of the mutations in the PACAP or PAC_1R locus on learning and memory function is also suggested. The ultimate mechanisms of learning and memory underlying PACAP will require further study.

REFERENCES

1. Arimura A. *Jpn J Physiol* 48, 301–331 (1998).
2. Vaudry D, Gonzalez BJ, Basille M *et al. Pharmacol Rev* 52, 269–324 (2000).
3. Hashimoto H, Nogi H, Mori K *et al. J Comp Neurol* 371, 567–577 (1996).
4. Quirk WG, Szlber PP and Booker R. *Nature* 277, 212–214 (1979).
5. Hashimoto H, Shintani N and Baba A. *Biochem Biophys Res Commun* 297, 427–432 (2002).
6. Otto C, Kovalchuk Y, Wolfer DP *et al. J Neurosci* 21, 5520–5527 (2001).
7. Telegdy G and Kokavszky K. *Brain Res* 874, 194–199 (2000).
8. Bliss TVP and Lomo T. *J Physiol* 232, 331–356 (1973).
9. Bliss TVP and Collingridge GL. *Nature* 361, 31–39 (1993).
10. Doyere V and Laroche S. *Hippocampus* 2, 39–48 (1992).
11. Kondo T, Tominaga T, Ichikawa M and Iijima T. *Neurosci Lett* 221, 189–192 (1997).
12. Roberto M and Brunelli M. *Learn Mem* 7, 303–311 (2000).
13. Matsuyama S, Namgung U and Routtenberg A. *Brain Res* 763, 127–130 (1997).
14. Hashimoto H, Shintani N, Nishino A *et al. J Neurochem* 73, 1810–1817 (2000).
15. Hashimoto H, Shintani N, Tanaka K *et al. Proc Natl Acad Sci USA* 98, 13355–13360 (2001).
16. Namgung U, Valcourt E and Routtenberg A. *Brain Res* 689, 85–92 (1995).
17. Brown TH and Zador AM. Hippocampus. In: Shepherd GM (ed.). *The Synaptic Organization of the Brain*. Oxford: Oxford University Press; 1990, pp. 346–388.
18. Shintani N, Mori W, Hashimoto H *et al. Reg Pept* 109, 45–48 (2002).
19. Gray SL, Cummings KJ, Jirik FR and Sherwood NM. *Mol Endocrinol* 15, 1739–1747 (2001).
20. Shioda S, Shuto Y, Somogyvári-Vigh A *et al. Neurosci Res* 28, 345–354 (1997).
21. Otto C, Zuschratter W, Gass P and Schütz G. *Mol Brain Res* 66, 163–174 (1999).
22. Sauvage M, Brabet P, Holsboer F *et al. Mol Brain Res* 84, 79–89 (2000).
23. Hannibal J. *J Comp Neurol* 453, 389–417 (2002).
24. Masuo Y, Matsumoto Y, Tokito F *et al. Brain Res* 611, 207–215 (1993).

Acknowledgements: We thank Dr Chikako Tanaka for her critical comments on the manuscript. This research was supported, in part, by a Grant-in-Aid for Scientific Research and Exploratory Research from the Ministry of Education, Culture, Sports, Science and Technology of Japan, and by grants from the New Energy and Industrial Technology Development Organization (NEDO) of Japan, Taisho Pharmaceutical Co. Ltd., AstraZeneca, and The Naito Foundation.

ELSEVIER

Brain Research 874 (2000) 194–199

BRAIN RESEARCH

www.elsevier.com/locate/bres

Research report

The action of pituitary adenylate cyclase activating polypeptide (PACAP) on passive avoidance learning. The role of transmitters

Gyula Telegdy*, Katalin Kokavszky

Institute of Pathophysiology, A. Szent-Györgyi Medical University, Semmelweis str. 1, POB 531, 6701 Szeged, Hungary

Accepted 13 June 2000

Abstract

In the present study, the action of PACAP 38 on one-way passive avoidance learning was investigated. PACAP-38 was administered into the lateral brain ventricle and the latency of the passive avoidance response was measured 24 h later. In order to study the possible roles of various neurotransmitters in mediating the action of PACAP on the consolidation of passive avoidance learning, the animals were pre-treated with receptor blockers in doses that per se proved to be ineffective. PACAP facilitated the learning, the consolidation of learning and the retrieval of the passive avoidance response. The following receptor blockers attenuated the action of PACAP on this consolidation: haloperidol, phenoxybenzamine, propranolol and methysergide. An antagonist of PACAP 38, PACAP 6-38, and also nitro-L-arginine (the latter blocks the enzyme nitric oxide synthase) thereby inhibiting the formation of NO from L-arginine, completely blocked the action of PACAP 38 on consolidation. The following receptor blockers were ineffective: naloxone, bicuculline and atropine. The presented data suggest that PACAP 38 is able to improve the learning and memory processes in a passive avoidance paradigm. In this action, the PACAP 38 receptor and NO are important mediators. Dopaminergic, alpha- and beta-adrenergic mediation and serotonin receptors modified the action of PACAP 38, but they are probably not of great importance. © 2000 Elsevier Science B.V. All rights reserved.

Theme: Neurotransmitters, modulators, transporters, and receptors

Topic: Peptides: anatomy and physiology

Keywords: PACAP; Passive avoidance learning; Neurotransmitter

1. Introduction

The pituitary adenylate cyclase activating polypeptide (PACAP) was isolated first from the ovine hypothalamus. It was found to contain 38 amino acids; a truncated form with 27 amino acid residues was later identified by Arimura and his co-workers [25,26]. These peptides stimulate cAMP accumulation in anterior pituitary cells, neurons and astrocytes [14]. PACAP 38 and 27 have been demonstrated in a number of brain regions, besides the hypothalamus: the septum, the thalamus, the amygdaloid complex, the hippocampus, various regions of the cortex and in the cerebellum [2,9,12,18,19,23,35]. At least two types of specific receptors have been isolated and characterized: the PACAP I and PACAP II receptors. The PACAP I receptor is specific for PACAP, while the PACAP II receptor can bind both PACAP and VIP. The PACAP I receptor is abundant in the brain [29,30]. The wide-ranging distribution of PACAP and its receptors in the brain [22] suggest that PACAP might have other important functions in the central nervous system in addition to its hypophysiotropic action.

PACAP given icv increases motor activity, counteracts reserpine-induced hypothermia [24], depresses the food [27] and water intake [8], and might be a potent controlling factor in the proliferation and/or differentiation of the granule cells in the cerebellum [4].

2. Methods

2.1. Animals and surgery

The experiments were carried out on male Wistar rats (LATI, Gödöllö, Hungary) weighing 140–170 g. The

*Corresponding author. Tel.: +36-62-420-651; fax: +36-62-420-651.
E-mail address: telegdy@paph.szote.u-szeged.hu (G. Telegdy).

0006-8993/00/$ – see front matter
PII: S0006-8993(00)02979-8

animals were kept and handled during the experiments in accordance with the instructions of the Albert Szent-Györgyi Medical University Ethical Committee for the Protection of Animals in Research. Five animals were housed per cage in a light- and temperature-controlled room (lights-on at 0600 and off at 1800 h 23°C) and had free access to food and water. For administration of the peptide, a stainless steel cannula with an external diameter of 0.7 mm was stereotaxically implanted into the right lateral brain ventricle, at a point 1.0 mm posterior, 1.5 mm lateral and 3.5 mm vertical, as described by Pellegrino et al. [28]. For anesthesia, barbital sodium was used (Nembutal 35 mg/kg ip). The cannula was fixed with dental cement and acrylic resin. The correct location of the cannula was checked by dissecting the brain following the experiments. Only experiments involving correctly located cannulae were evaluated. All experiments were performed in the morning period.

2.2. Materials

PACAP 38 and PACAP 6-38 were purchased from Bachem Calif. and were administered icv in a volume of 2 ul in different doses. For blockade of the enzyme nitric oxide synthase, nitro-L-arginine (Sigma) was used in a dose of 5 ug in 2 ul volume, injected into the lateral brain ventricle in freely-moving rats via a chronically implanted cannule, 1 week following implantation. The dose was selected on the basis of earlier experience [34].

The following receptor blockers were used: propranolol hydrochloride (ICI Ltd., Macclesfield, UK), 10 mg/kg ip; naloxone hydrochloride (Endo Lab. Inc. New York, USA), 0.3 mg/kg; bicuculline methiodide (Sigma, St. Louis, USA), 1 mg/kg ip, nitro-L-arginine (*N*-w-nitro-L-arginine, N-NA, Sigma-Aldrich, Budapest, Hungary), 5 ug icv); haloperidol (G. Richter, Budapest, Hungary), 10 ug/kg ip; atropine sulphate (EGYS, Budapest, Hungary), 2 mg/kg ip; phenoxybenzamine hydrochloride (Smith, Klein and French, Herts, UK), 2 mg/kg ip; and methysergide hydrogenmaleate (Sandoz, Basle, Switzerland), 5 mg/kg ip. The doses of the receptor blockers were selected on the basis of earlier experience as being effective when administered with other neuropeptides,but not affecting the paradigm per se [31].

2.3. Passive avoidance behavior

For the study the passive avoidance learning, the method of Ader et al. was used [1]. Briefly, the animals were trained in a one-trial learning passive avoidance apparatus, which consisted of an illuminated platform attached to a dark box. On the first day, the animals were trained to move from the illuminated platform to the dark compartment three times. On the following day, after the second entry, the animal in the dark compartment received an unavoidable shock (0.5 mA for 2 s), which was delivered through the grid floor of the compartment. The animals were tested 24 h later.

In order to study the action of the peptide, PACAP was given immediately after the learning trial (consolidation) in a dose of 500 ng or 1 ug and the animals were tested 24 h later, before the learning trial (learning) and 30 min before the 24-h testing (retrieval).

2.4. Statistical analysis

For statistical evaluation of the data, the one-way analysis of variance (ANOVA) test followed by the TUKEY test for multiple comparisons with unequal cell size was used. A probability level of 0.05 was accepted as statistically relevant.

3. Results

Effects of PACAP on the consolidation of passive avoidance learning are demonstrated in Fig. 1. The doses of 500 ng and 1 ug of PACAP given icv immediately after the learning trial, with tests 24 h later, increased the passive avoidance response in a dose-response manner (500 ng and 1 ug, $P<0.05$ vs. control, $F(3,66)=3.49$).

In order to study the action of PACAP on learning, PACAP was administered icv in a dose of 1 ug 30 min before the learning trial (Fig. 2). PACAP 38 increased the latency of entry, and facilitated the learning processes ($P<0.05$ vs. control, $F(1,42)=25.02$).

When the action of PACAP on the retrieval was followed, the peptide (1 ug) was administered 30 min before the 24-h testing. The PACAP pretreatment lengthened the passive avoidance response, and thereby facilitated the retrieval processes ($P<0.05$ vs. the control, $F(1,42)=35.11$, Fig. 3).

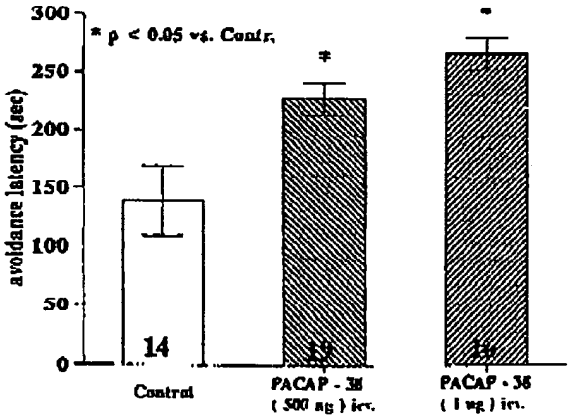

Fig. 1. The effects different doses of PACAP 38 on the consolidation of learning of passive avoidance behavior. The values are mean±S.E.M. Number in bars represents the number of animals used.

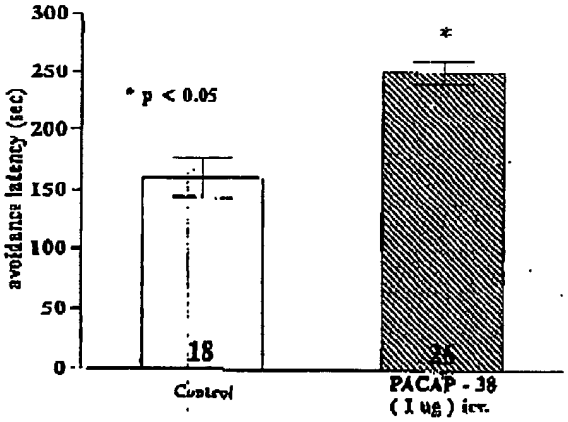

Fig. 2. The effects of PACAP 38 on the learning of passive avoidance behavior. The values are mean±S.E.M. Number in bars represents the number of animals used.

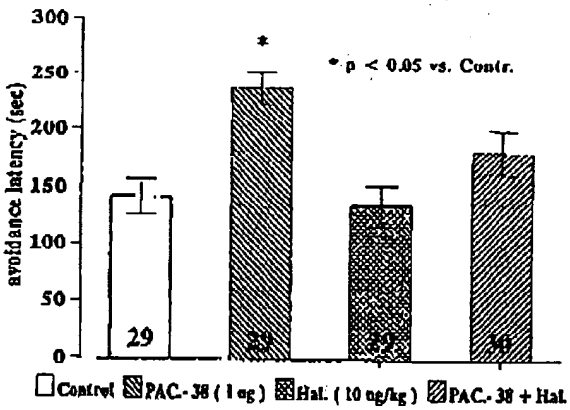

Fig. 4. The effects of haloperidol (10 ug/kg ip) pretreatment on the action of PACAP 38 on the consolidation of passive avoidance behavior. The values are mean±S.E.M. Number in bars represents the number of animals used. Abbrevation: PAC.-38=PACAP 38, Hal.=haloperidol.

In previous studies we have demonstrated that a number of neurotransmitters can be involved in the action of different neuropeptides [31]. In order to study the involvement of dopaminergic transmission in the consolidation of passive avoidance learning, the animals were pretreated with haloperidol (10 ug/kg ip) immediately after the learning trials, 30 min before PACAP administration. Haloperidol attenuated, but was unable to block the action of PACAP (Fig. 4, $F(3,113)=7.84$), PACAP $P<0.05$ vs. the control. There was no significant difference between the PACAP and PACAP+haloperidol groups and no significant difference between the control and PACAP+haloperidol groups. Thus, dopaminergic mediation is only partly involved in the action of PACAP.

The same was true for phenoxybenzamine (2 mg/kg ip), PACAP vs. the control and phenoxybenzamine ($P<0.05$, $F(3,72)=3.48$). The results of the combined treatment PACAP+phenoxybenzamine, did not differ statistically from those for the control and PACAP (Fig. 5).

Propranolol a beta-adrenergic receptor blocker (10 mg/kg ip), displayed a similar profile. PACAP vs. the control $P<0.05$ ($F(3,72)=3.48$). No significant alteration was observed between PACAP+propranolol and the control and PACAP+propranolol and PACAP (Fig. 6).

Methysergide (5 mg/kg ip) also attenuated the action of PACAP, but was unable to block the action of PACAP (PACAP vs. the control $P<0.05$, $F(3,82)=5.38$). No significant alteration was observed between PACAP+methysergide and the control and PACAP+methysergide and PACAP (Fig. 7).

The antagonist of PACAP 38, PACAP 6-38 (4 ug icv. before the PACAP 38) completely blocked the action of PACAP 38 on consolidation (PACAP 38+PACAP 6-38 vs.

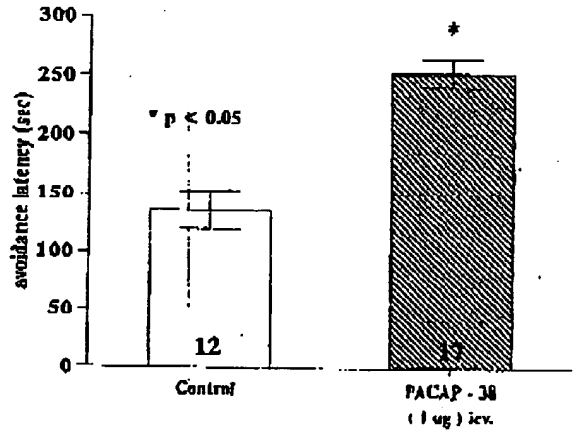

Fig. 3. The effects of PACAP 38 on the retrieval of passive avoidance behavior. The values are mean±S.E.M. Number in bars represents the number of animals used.

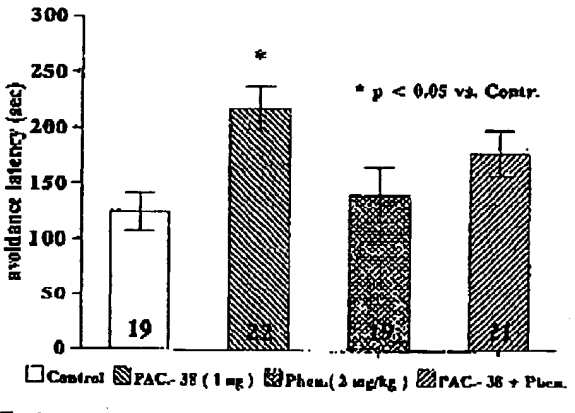

Fig. 5. The effects of phenoxybenzamine (2 mg/kg) pretreatment on the action of PACAP 38 on the consolidation of passive avoidance behavior. The values are mean±S.E.M. Number in bars represents the number of animals used. Abbrevation: PAC.-38=PACAP 38, Phen.= phenoxybenzamine.

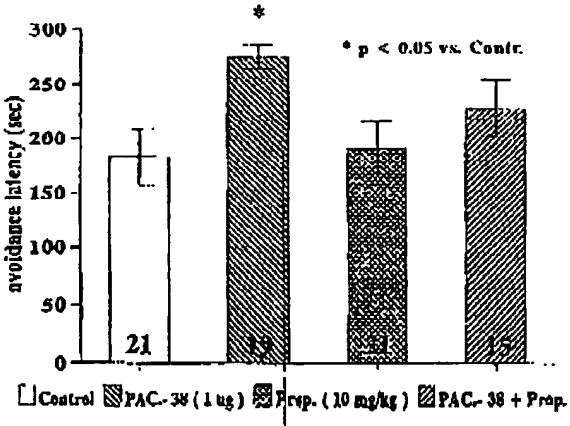

Fig. 6. The effects of propranolol (10 mg/kg) pretreatment on the action of PACAP 38 on the consolidation of passive avoidance behavior. The values are mean±S.E.M. Number in bars represents the number of animals used. Abbrevation: PAC.-38=PACAP 38, Prop=propranolol.

PACAP 38, $P<0.05$, $F(3,148)=11.74$, Fig. 8), proving that PACAP 38 does indeed act on the PACAP receptor.

We tested whether the action of PACAP can be blocked by nitro-L-arginine. The dose of nitro-L-arginine was selected on the basis of previous experiments: 5 ug was given icv (34). In order to establish whether, by blocking the NO synthase, nitro-L-arginine can prevent the action of PACAP on the consolidation of passive avoidance learning, the animals were pretreated with nitro-L-arginine immediately after the learning trial and PACAP was given 30 min later. The action of 1 ug PACAP was blocked by NO synthase inhibition (PACAP+nitro-L-arginine vs. PACAP, $P<0.05$, $F(3,66)=3.49$, Fig. 9). NO may act as a possible mediator of PACAP action, which can be involved in learning and memory processes.

Pretreatment with atropine (2 mg/kg ip), naloxone (0.3

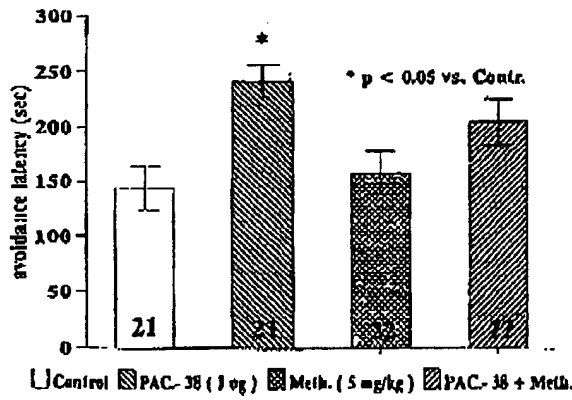

Fig. 7. The effects of methysergide (5 mg/kg) pretreatment on the action of PACAP 38 on the consolidation of passive avoidance behavior. The values are mean±S.E.M. Number in bars represents the number of animals used. Abbrevation: PAC.-38=PACAP 38, meth=methysergide.

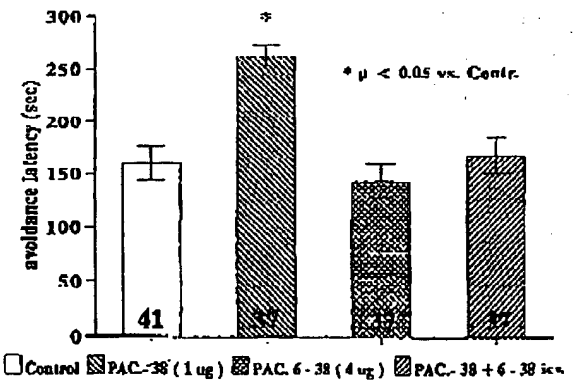

Fig. 8. The effects of PACAP 6-38 (4 ug icv) pretreatment on the action of PACAP 38 on the consolidation of passive avoidance behavior. The values are mean±S.E.M. Number in bars represents the number of animals used. Abbrevation: PAC-38=PACAP 38, PAC. 6-38=PACAP 6-38.

mg/kg ip) or bicuculline (1 mg/kp ip) was ineffective (data are not shown).

4. Discussion

It was concluded that PACAP given icv is able to improve the learning, the consolidation of learning and the retrieval of learning in a passive avoidance paradigm. The action is mediated by the PACAP receptor. The NO synthase inhibitor nitro-L-arginine prevents the facilitatory action of PACAP on consolidation processes, demonstrating that NO could be an important mediator in the action of PACAP.

In the facilitatory action of PACAP on consolidation, no cholinergic, opiate or GABA-ergic mediation is involved.

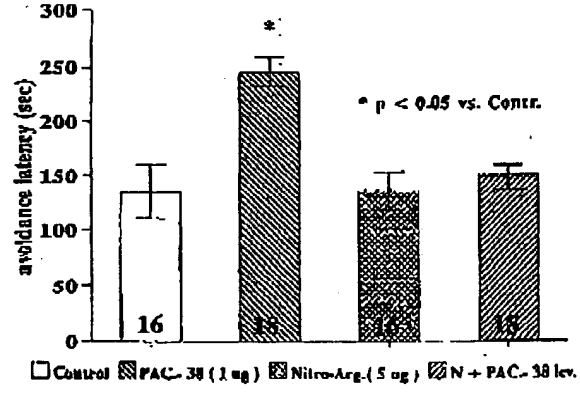

Fig. 9. The effects of nitro-L-arginine (5 ug icv) pretreatment on the action of PACAP 38 on the consolidation of passive avoidance behavior. The values are mean±S.E.M. Number in bars represents the number of animals used. Abbrevation: PAC.-38=PACAP 38. Nitro-Arg. N=Nitro-L-arginine.

The fact that dopaminergic, alpha- and beta-adrenergic and serotonergic receptor blockers partly blocked the action of PAPAC suggests, that these transmitters might be involved in some component of learning and memory action of PACAP (motivation, arousal, fear etc.), but their roles are probably not highly significant.

That PACAP might be involved in learning processes was indicated in the work of Yamaguchi et al. [36], who demonstrated that scopolamine induced-impairment in radial maze learning could be corrected by treatment with PACAP 1-27.

The question arises of whether PACAP acts via the involvement of neurotransmitters, or whether other mediators (e.g. neuropeptides), could also be involved in this action. It has been shown that PACAP can stimulate ACTH secretion [13], increase the immunoreactivity of CGRP in vitro in the dorsal root ganglion [20], and stimulate atrial natriuretic peptide (ANP) secretion from cultured neonatal rat myocardiocytes [5].

We have revealed that these peptides can also improve learning and memory formation in an avoidance task for ACTH [3], CGRP [15], and ANP [6]. All these peptides can improve the memory and learning processes. However there are both similarities and dissimilarities in their actions.

ACTH can facilitate passive avoidance behavior [21], while it delays the extinction of active avoidance behavior [3]. Most of the behavioral data indicate that dopaminergic transmission could be involved in this action [10,11,32,33]. In our experiments, the cholinergic and dopaminergic systems are also involved in the extinction of active avoidance behavior since this action can be blocked by atropine and haloperidol [3]. When the evidence is considered overall, it might be concluded that ACTH is most probably not involved in the action of PACAP, since haloperidol has only attenuating action, while atropine did not block the action of PACAP in the paradigm used.

As regards the possible involvement of CGRP in mediation of the action of PACAP, CGRP can also improve learning and memory formation and retrieval processes in the same passive avoidance paradigm [15]. Propranolol, naloxone, methysergide and nitro-arginine were effective in blocking the action of CGRP, whereas phenoxybenzamine, bicuculline and atropine were ineffective [16,17]. If we compare the actions of PACAP and CGRP, most of the ineffective transmitters, such as atropine and bicuculline, were ineffective in both cases, while naloxone was effective against CGRP and ineffective against PACAP, and propranolol and methysergide displayed weak action against PACAP, but a strong action against CGRP. Haloperidol exhibited weak action against PACAP and no action against CGRP. These findings might indicate that CGRP could be partly involved in mediation of the action of PACAP.

As regards the action of ANP, ANP acted only on learning and the consolidation of memory processes, but had no action in retrieval, in contrast with PACAP [7]. The transmitter involvement in the ANP actions of haloperidol, atropine blocked the action of ANP, while phenoxybenzamine, propranolol, naloxone, bicuculline and methysergide were ineffective [7]. Since this profile differs very much from that of PACAP, it is not likely that the action of PACAP is mediated by ANP.

Acknowledgements

This work was supported by OTKA (T-022230, ETT (T-02670/96), FKFP (0091/1997) and MTA-AKP (96-330 3,2).

References

[1] R. Ader, J.A.W.M. Weijnen, P. Moleman, Retention of a passive avoidance response as a function of the intensity and duration of electric shock, Psychon. Sci. 26 (1972) 125–128.

[2] A. Arimura, A. Somogyvári-Vigh, A. Miyata, K. Mizuno, D.H. Coy, C. Kitada, Tissue distribution of PACAP as determined by RIA: highly abundant in the rat brain and testes, Endocrinology 129 (1991) 2787–2789.

[3] M. Balázs, G. Telegdy, Effects of receptor blockers on ACTH-induced changes in extinction of active avoidance reflex in rat, Pharmacol. Biochem. Behav. 31 (1989) 515–518.

[4] M. Basile, B.J. Gonzales, P. Leroux, L. Jeandel, A. Fournier, H. Vaudry, Localization and characterization of PACAP receptors in the rat cerebellum during development: evidence for a stimulatory effect of PACAP on immature cerebellar granule cells, Neuroscience 57 (1993) 329–338.

[5] I. Basler, M. Knn, W. Müller, W.G. Forssmann, Pituitary adenylate cyclase-activating polypeptide stimulates cardiodilatin/atrial natriuretic peptide (CDD/ANP-(99-126)) secretion from cultured neonatal rat myocardiocytes, Eur. J. Pharmacol. Mol. Pharm. 291 (1995) 335–342.

[6] A. Bidzseranova, J. Gueron, B. Penke, G. Telegdy, The effects of atrial natriuretic peptide on active avoidance behavior in rats. The role of transmitter, Pharmacol. Biochem. Behav. 40 (1991) 61–64.

[7] A. Bidzseranova, G. Telegdy, B. Penke, The effects of atrial natriuretic peptide on passive avoidance behaviour in rats, Br. Res. Bull. 26 (1991) 177–180.

[8] W.T. Chance, H. Thompson, I. Thomas, J.E. Fischer, Anorectic and neurochemical effects of pituitary adenylate cyclase activating polypeptide in rats, Peptides 16 (1995) 1511–1516.

[9] A. Couvin, P. Robberecht, P. De Neef, P. Gourlet, A. Vandermeers, M.C. Vandermeers-Piret, J. Christophe, Properties and distribution of receptors for pituitary adenylate cyclase activating peptide (PACAP) in rat brain and spinal cord, Regul. Pept. 35 (1991) 161–163.

[10] M. Fekete, E. Stark, J.P. Herman, M. Palkovits, ACTH-induced changes in the in the transmitter amine concentration of individual brain nuclei of the rat, in: E. Usdin (Ed.), Catecholamines and Stress, Pergamon Press, Oxford, 1976, pp. 69–75.

[11] M. Fekete, E. Stark, J.P. Herman, M. Palkovits, B. Kanicska, Catecholamine concentration of various brain nuclei of the rat as affected by ACTH and corticosterone, Neurosci. Lett. 10 (1978) 153–158.

[12] M.A. Ghatei, K. Takahashi, Y. Suzuki, J. Gardiner, P.M. Jones, S.R. Bloom, Distribution, molecular characterization of pituitary adenylate cyclase-activating polypeptide and its precursor encoding

messenger RNA in human and rat tissues, J. Endocrinol. 136 (1993) 159–166.
[13] G.R. Hart, H. Gowing, J.M. Burnn, Effects of a novel hypothalamic peptide, pituitary adenylate cyclase-activating polypeptide, on pituitary hormone release in rats, J. Endocrinol. 134 (1992) 33–41.
[14] G. Katsuura, R.R. Dahl, A. Miyata, A. Arimura, A novel hypothalamic neuropeptide with 38 residues (PACAP 38) stimulates adenylate cyclase activity in pituitary cells, neurons and astrocytes, Soc. Neurosci. Abstr. 15 (1989) 1277.
[15] A. Kovács, G. Telegdy, Effects of intracelebroventricular administration of calcitonin gene-related peptide on passive avoidance behaviour in rats, Neuropeptides 23 (1992) 51–54.
[16] A. Kovács, G. Telegdy, The involvement of nitric oxide (NO) in the CGRP-induced behavior of rats, Peptides 17 (1996) 1183–1187.
[17] A. Kovács, G. Telegdy, Effect of calcitonin gene-related peptide on passive avoidance behavior in rats, Ann. NY Acad. Sci. 657 (1992) 543–545.
[18] K. Köves, A. Arimura, T.G. Görcs, A. Somogyvári-Vigh, Comparative distribution of immunoreactive pituitary adenylate cyclase activating polypeptide and vasoactive intestinal polypeptide in rat forebrain, Neuroendocrinology 54 (1991) 159–169.
[19] K. Köves, A. Arimura, A. Somogyvári-Vigh, S. Vigh, J. Miller, Immunocytochemical demonstration of a novel hypothalamic peptide, pituitary adenylate cyclase activating polypeptide (PACAP), in the ovine hypothalamus, Endocrinology 127 (1990) 264–271.
[20] M. Lioudyno, Y. Skoglosa, N. Takey, D. Lindholm, Pituitary adenylate cyclase-activating polypeptide (PACAP) protects dorsal root ganglion neurones from death and induces calcitonin gene-related peptide (CGRP) immunoreactivity in vitro, J. Neurosci. Res. 51 (1998) 243–256.
[21] K. Lissák, E. Endröczi, P. Medgyesi, Somatisches verhalten und nebennierenrinde unigkeit, Pflügers Arch. 117 (1957) 265–273.
[22] Y. Masuo, T. Ohtaki, Y. Masuda, Y. Nagai, M. Suno, M. Tsudo, M. Fujino, Autoradiographic distribution of pituitary adenylate cyclase activating polypeptide (PACAP) binding sites in the rat brain, Neurosci. Lett. 126 (1991) 103–106.
[23] Y. Masuo, N. Suzuki, H. Matsumoto, F. Tokito, Y. Matsumoto, M. Tsuda, M. Fujino, Regional distribution of pituitary adenylate cyclase activating polypeptide (PACAP) in the rat central nervous system as determined by sandwich-enzyme immunoassay, Brain Res. 602 (1993) 57–63.
[24] J. Masuo, J. Noguchi, S. Morita, Y. Matsumoto, Effects of intracerebroventricular administration of pituitary adenylate cyclase-activating polypeptide (PACAP) on the motor activity and reserpine-induced hypothermia in murines, Brain Res. 700 (1995) 219–226.
[25] A. Miyata, A. Arimura, R.R. Dahl, N. Minamino, A. Uehara, L. Jiang, M.D. Culler, D.H. Coy, Isolation of a novel 38 residue-hypothalamic polypeptide which stimulates adenylate-cyclase in pituitary cells, Biochem. Biophys. Res. Commun. 164 (1989) 567–574.
[26] A. Miyata, L. Jiang, R.R. Dahl, C. Kitada, K. Kubo, M. Fujino, N. Minamino, A. Arimura, Isolation of a neuropeptide corresponding to the N-terminal 27 residues of the pituitary adenylate cyclase activating polypeptide with 38 residues (PACAP38), Biochem. Biophys. Res. Commun. 170 (1990) 643–648.
[27] J.E. Morley, M. Horowitz, M.K. Morley, J.F. Flood, Pituitary adenylate cyclase activating polypeptide (PACAP) reduces food intake in mice, Peptides 13 (1992) 1133–1135.
[28] L.J. Pellegrino, A.S. Pellegrino, A.J. Cushman, A Stereotactic Atlas of the Rat Brain, Plenum Press, New York, 1979.
[29] P. Robberecht, M.-C. Woussen-Colle, P. DeNeff, P. Gourlet, P.L. Buscail, A. Vandermeers, M.-C. Vandermeers-Piret, J. Christophe, The two forms of the pituitary adenylate cyclase activationg polypeptide (PACAP (1-27) and PACAP (1-38) interact with distinct receptors on rat pancreatic AR 4-2J cell membranes, FEBS Lett. 286 (1991) 133–136.
[30] B.D. Shivers, T.J. Görcs, P.E. Gouschall, A. Arimura, Two high affinity bindings sites for pituitary adenylate cyclase-activating polypeptide have different tissue distributions, Endocrinology 128 (1991) 3055–3065.
[31] G. Telegdy, Neuropeptides and brain function, in: T.B. van Wimersma Greidanus (Ed.), Frontiers of Hormone Research, Vol. 15, Karger, Basel, 1984, pp. 1–332.
[32] G. Telegdy, G.L. Kovács, Role of monoamines in mediating the action of hormones on learning and memory, in: M. Brazier (Ed.), Brain Mechanisms in Memory and Learning: From Single Neuron to Man, IBRO Monogr. Ser, Vol. 4, Raven Press, New York, 1979, pp. 249–268.
[33] G. Telegdy, G.L. Kovács, Role of monoamines in mediating the action of ACTH, vasopressin and oxytocin, in: R. Collu, A. Barbeau, J.R. Ducharme, J. Rochefort (Eds.), Central Nervous System Effects of Hypothalamic Hormones and Other Peptides, Raven Press, New York, 1979, pp. 189–205.
[34] G. Telegdy, G.L. Kovács, A. Nyerges, Action of C-type natriuretic peptide (CNP) on passive avoidance learning in rats: involvement of transmitters, Eur. J. Neurosci. 11 (1999) 3302–3306.
[35] S. Vigh, A. Arimura, K. Köves, A. Somogyvári-Vigh, J. Sitton, C.D. Fermin, Immunocythochemical localization of the neuropeptide, pituitary adenylate cyclase activating polypeptide (PACAP), in human and primate hypothalamus, Peptides 12 (1991) 313–318.
[36] Y. Yamaguchi, M. Higashi, M. Nishio, H. Kobayashi, Effects of PACAP, VIP and their peptide fragments on scopolamine-induced impaired performance and on the chat activity in the brain of rats, Neuroendocrinol. Lett. 18 (1997) 7–14.

The Journal of Neuroscience, August 1, 2001, 21(15):5520–5527

Impairment of Mossy Fiber Long-Term Potentiation and Associative Learning in Pituitary Adenylate Cyclase Activating Polypeptide Type I Receptor-Deficient Mice

Christiane Otto,[1] Yury Kovalchuk,[2] David Paul Wolfer,[4] Peter Gass,[1,5] Miguel Martin,[6] Werner Zuschratter,[7] Hermann Josef Gröne,[3] Christoph Kellendonk,[1,8] François Tronche,[1] Rafael Maldonado,[6] Hans-Peter Lipp,[4] Arthur Konnerth,[2] and Günther Schütz[1]

Divisions of [1]Molecular Biology of the Cell and [2]Experimental Pathology, German Cancer Research Center, 69120 Heidelberg, Germany, [3]Department of Physiology, Ludwig Maximilians University München, 80802 München, Germany, [4]Institute of Anatomy, University of Zürich, 8057 Zürich, Switzerland, [5]Central Institute of Mental Health, 68159 Mannheim, Germany, [6]Department of Neuropharmacology, University Pompeu Fabra, 08003 Barcelona, Spain, [7]Leibniz Institute for Neurobiology, 39118 Magdeburg, Germany, and [8]Center for Neurobiology and Behavior, Howard Hughes Medical Institute, Columbia University, New York, New York 10032

The pituitary adenylate cyclase activating polypeptide (PACAP) type I receptor (PAC1) is a G-protein-coupled receptor binding the strongly conserved neuropeptide PACAP with 1000-fold higher affinity than the related peptide vasoactive intestinal peptide. PAC1-mediated signaling has been implicated in neuronal differentiation and synaptic plasticity. To gain further insight into the biological significance of PAC1-mediated signaling *in vivo*, we generated two different mutant mouse strains, harboring either a complete or a forebrain-specific inactivation of *PAC1*.

Mutants from both strains show a deficit in contextual fear conditioning, a hippocampus-dependent associative learning paradigm. In sharp contrast, amygdala-dependent cued fear conditioning remains intact. Interestingly, no deficits in other hippocampus-dependent tasks modeling declarative learning such as the Morris water maze or the social transmission of food preference are observed. At the cellular level, the deficit in hippocampus-dependent associative learning is accompanied by an impairment of mossy fiber long-term potentiation (LTP). Because the hippocampal expression of *PAC1* is restricted to mossy fiber terminals, we conclude that presynaptic PAC1-mediated signaling at the mossy fiber synapse is involved in both LTP and hippocampus-dependent associative learning.

Key words: PACAP type I receptor; knock-out mice; fear conditioning; synaptic plasticity; LTP; mossy fiber

The pituitary adenylate cyclase activating polypeptide (PACAP) type I receptor PAC1 is a G-protein-coupled receptor that can activate several second messengers, most importantly the adenylate cyclase–protein kinase A (PKA) signal transduction pathway (Christophe, 1993). PAC1 binds the strongly conserved neuropeptide PACAP with a 1000-fold higher affinity than its related peptide vasoactive intestinal peptide (VIP) (Shivers et al., 1991). Unlike PACAP type II receptors VPAC1 and VPAC2, which are strongly expressed in peripheral tissues such as lung, liver, and the gastrointestinal tract (Ishihara et al., 1992; Lutz et al., 1993), PAC1 is predominantly expressed in the CNS. Especially the neocortex, the limbic system, and the brainstem exhibit a strong expression of *PAC1* mRNA (Hashimoto et al., 1996a; Otto et al., 1999). PAC1 has been implicated in neurotransmission, neurotrophic actions, neuronal differentiation, and synaptic plasticity (Arimura, 1998). Interestingly, within the hippocampus, PAC1 expression is restricted to the granule cells of the dentate gyrus, and the PAC1 protein is localized presynaptically in hippocampal mossy fiber terminals (Otto et al., 1999). There is, thus, a remarkable coincidence of the presynaptic expression of PAC1 and the well established role of calcium and cAMP in synaptic transmission and long-term potentiation (LTP) at hippocampal mossy fiber terminals (Huang et al., 1994; Weisskopf et al., 1994). This coincidence and the finding that *Drosophila* harboring a mutation in the PACAP-related gene *amnesiac* display deficits in associative learning (Quinn et al., 1979) suggest a possible role of PAC1 in learning and memory.

Two types of information storage have been identified in the mammalian brain: declarative and nondeclarative memory and learning. In contrast to the phylogenetically younger declarative learning, associative learning (a subtype of nondeclarative learning) is already well developed in invertebrates (Milner et al., 1998). The hippocampus seems to play a pivotal role in the generation of long-term memory in almost all declarative (Milner et al., 1998) paradigms and at least one associative learning model, i.e., contextual fear conditioning (Kim and Fanselow, 1992; Phillips and LeDoux, 1992). It is generally accepted, although not yet formally demonstrated, that activity-dependent long-lasting changes in synaptic strength, particularly LTP, represent the cellular basis for the consolidation of long-term memory (Swanson et al., 1982). Within the hippocampus three types of excitatory synapses using glutamate as neurotransmitter are known: the perforant-path synapse, the mossy fiber synapse, and

Received Dec. 5, 2000; revised May 7, 2001; accepted May 8, 2001.

This work was supported by the European Commission, the Deutsche Forschungsgemeinschaft, the Fonds der Chemischen Industrie, the Bundesministerium für Bildung und Forschung, and the Volkswagenstiftung. We are grateful to H. Kern, A. Klewe-Nebenius, K. Anlag, R. Klären, and I. Bornfeldt for technical assistance and to Dr. T. Mantamadiotis for carefully reading this manuscript.

Correspondence should be addressed to Dr. Günther Schütz, Molekularbiologie der Zelle, Im Neuenheimer Feld 280, 69120 Heidelberg, Germany. E-mail: g.schuetz@dkfz-heidelberg.de.

the Schaffer collateral LTP at the Schaffer collateral and the perforant path synapses is initiated postsynaptically by an activation of NMDA receptors, which leads to a postsynaptic calcium rise and activation of calcium–calmodulin-dependent kinase II (Bliss and Collingridge, 1993). LTP at the mossy fiber synapse is distinctly different from LTP at the other hippocampal synapses. It is NMDA receptor-independent and requires a presynaptic calcium rise (Nicoll and Malenka, 1995), which leads via calmodulin to an activation of adenylate cyclases and PKA (Huang et al., 1994; Weisskopf et al., 1994). To address the role of PAC1-mediated signaling in synaptic plasticity and learning and memory, we generated two different mutant mouse lines harboring either a complete or a forebrain-specific inactivation of PAC1.

MATERIALS AND METHODS

Generation of mice. We modified the *PAC1* locus in embryonic stem (ES) cells (ET14/1) as described (Gu et al., 1994). The targeting vector was constructed from isogenic DNA (Kaestner et al., 1994). The upstream *loxP* site, together with an additional *XbaI* site was introduced into the intron preceding exon 11 using overlap PCR. The targeting vector consisted of a 3.5 kb 5′-homology arm carrying exons 7–10 of the *PAC1* gene, followed by a 0.35 kb *BamHI/HindIII* fragment encompassing the upstream *loxP* site and exon 11. The selection cassette flanked by two *loxP* sites was introduced downstream of the *BamHI/HindIII* fragment. The 3′-homology arm was a 4.5 kb *HindIII* fragment. After transfection of ES cells, G418-resistant clones were analyzed by Southern blot using probes from outside the homology arms. Homologously recombined clones (frequency of homologous recombination was 12%) were transiently transfected with a Cre expression plasmid (20 μg), and subclones were selected in the presence of ganyclovir (1 μM). Mice carrying the *PAC1*$^{-}$ or *PAC1*$^{hip-}$ allele were derived by blastocyst injection.

For generation of CaMKCre2 mice, nlsCre has been cloned into a CaMKIIα-vector, as described previously (Kellendonk et al., 1999). Linearized pMM403-Cre insert DNA was injected into the pronuclei of C57BL/6 oocytes, and several transgenic lines were obtained. In the CaMKCre2 line, Cre recombinase expression pattern was defined using an anti-Cre recombinase antibody (Kellendonk et al., 1999). In 30% of the *PAC1*^{CaMKCre2} mice, mosaic inactivation of the Cre recombinase transgene was observed. Those mice were identified *postmortem* immunohistochemically and excluded from the results.

RNase protection analysis and in situ hybridization. RNase protection analysis and *in situ* hybridization were performed as described previously (Otto et al., 1999). Probes used in RNase protection analysis were: PAC1 [nucleotides (nt) 637–1037 of the murine PAC1 cDNA] (Hashimoto et al., 1996b), VPAC1 (nt 1–232 of the murine VPAC1 cDNA) (Johnson et al., 1996), and VPAC2 (nt 106–446 of the murine VPAC2 cDNA) (Inagaki et al., 1994).

Electrophysiology. Hippocampal slices (300 μm thick) were prepared from 4- to 6-week-old mice. Slices were incubated at 33°C in oxygenated standard solution for at least 1 hr before transferring them into the recording chamber. The standard solution contained (in mM): 125 NaCl, 2.5 or 3.5 KCl, 2 $CaCl_2$, 1.2 $MgCl_2$, 1.25 NaH_2PO_4, 26 $NaHCO_3$, and 20 glucose, bubbled with 95% O_2 and 5% CO_2. Whole-cell recordings were performed in the presence of bicuculline (10 μM). For the recordings of EPSCs at mossy fiber synapses (MF-EPSCs), the concentration of $CaCl_2$ was raised to 3 mM, and 100 μM DL-AP-5 and 0.3 μM CNQX were added to prevent epileptiform activity. The MF-EPSCs were recorded at a holding potential of −70 mV. During the test period, mossy fibers were stimulated every 20 sec using glass pipettes (containing 1 M NaCl) that were placed in stratum lucidum. LTP of the MF-EPSC was produced by a train lasting 5 sec at 25 Hz, administered at control stimulus intensity (Castillo et al., 1997). At the end of the recordings (2*S*,1′*R*,2′*R*,3′*R*)-2-(2,3-dicarboxycyclopropyl)-glycine (DCG-IV; 1 μM), a specific agonist of the metabotropic glutamate receptors (mGluRs) of the group 2/3 subtype specifically expressed in mossy fiber terminals but not at associational–commissural synapses (Yokoi et al., 1996; Castillo et al., 1997), was added to the bath to assess the mossy fiber component of the recorded EPSC. In addition, MF inputs were identified by their distinct properties concerning paired-pulse facilitation (PPF), frequency facilitation and the fast rise time of the EPSCs (Claiborne et al., 1993; Salin et al., 1996; Yeckel et al., 1999). To evoke EPSCs in the granule cells, the glass electrode was positioned in the outer third of the molecular layer of the dentate gyrus, thereby stimulating preferentially the lateral perforant path (LPP). The test stimuli were delivered every 15 sec, and the EPSCs were recorded at a holding potential of −70 to −80 mV. LTP was induced by five bursts of stimuli (10 sec at 100 Hz) delivered at interval of 15 sec, whereas the whole-cell amplifier was switched to the current-clamp mode, and the holding voltage was set to −50 mV.

Whole-cell recordings were performed using an EPC-9 patch-clamp amplifier (Heka, Lambrecht, Germany). The pipette solution contained (in mM): 140 K-gluconate, 10 NaCl, 2 Mg-ATP, 2 Na_2-ATP, 0.4 Na_2-GTP, 10 K-HEPES, 10 phosphocreatine, and 0.1 Oregon Green 488 BAPTA-1. The pH was adjusted to 7.3 with KOH. The fluorescent indicator Oregon Green 488 BAPTA-1 was included to acquire confocal images of the recorded CA3 pyramidal cells, confirming their identity. The pipette resistance ranged from 3.5 to 7.5 MΩ, and the series resistance from 11 to 25 MΩ for recording from CA3 cells and 25 to 50 MΩ for recordings from granule cells. No series resistance compensation was applied. The recordings from the granule cells with a series resistance <25 MΩ were discarded for the reason that the induction of LTP was not reliable, perhaps reflecting the "washout of LTP" in whole-cell configuration. The experiments were performed either at room temperature [21–25°C; MF-LTP, MF-PPF, and MF- post-tetanic potentiation (PTP)] or at 30–32°C (PP-LTP). PPF was defined as the percentage ratio of the EPSC in response to the second versus that obtained with the first stimulus. The interstimulus interval was 60 msec. PTP was measured as a ratio of the mean EPSC amplitude averaged over the first minute after the conditioning tetanus and the mean amplitude of the control EPSC recorded before the tetanic stimulation.

Behavioral studies. We matched mutant and control mice for sex and age and housed littermates together. Data were analyzed by Student's *t* test, and results are depicted as mean ± SEM. For direct comparison of both mutant mouse strains, all experiments of this study were performed on the same genetic background, i.e., 75% C57BL/6/25% 129 Ola.

Social transmission of food preference. The social transmission of food preference was performed as described previously (Gass et al., 1998). Training and testing of mice was comprised of three main stages. First, a demonstrator mouse was allowed to eat powdered ground chow scented with either cinnamon (1% w/w) or cocoa (2% w/w). Second, the demonstrator mouse and littermate observer mice (memory-tested mice) were allowed to freely interact for 10 min. In the third phase, observer mice were tested for food preference 24 hr after the interaction session. Each mouse was given a free choice between two food cups with cinnamon or cocoa, respectively, for 2 hr. Afterward, the amounts of cued and noncued food eaten were determined.

Morris water maze. A white Plexiglas circular pool of 150 cm diameter and 50 cm height was filled with water (16 cm deep, 24–26°C) and made opaque by the addition of milk (Gass et al., 1998). Distant visual cues for navigation were available on the walls of the room illuminated by diffuse light (12 lux). A wire mesh platform (16 × 16 cm) was placed 0.5 cm below the water surface, at 35 cm from the wall of the pool. The swim paths of the mice were recorded using a video camera suspended above the center of the pool and were fed to an electronic imaging system recording the *x-y* coordinates (Noldus EthoVision 1.90). The recorded paths were analyzed as described previously (Gass et al., 1998). During the acquisition phase, animals had two training trials per day (with an interval of 1 min) over a period of 14 consecutive days. The 1 min intertrial interval was spent on the platform. If an animal did not find the platform in the first trial, it was placed on it after 1 min. The probe trial (free swimming without the platform in the pool) was performed on days 10 and 15. Data were analyzed by a repeated two-way ANOVA.

Fear conditioning. The conditioning system (TSE, Bad Homburg, Germany) consisted of a soundproof box (58 × 30 × 27 cm) with a gray interior, a 12 V light at the ceiling, and a Plexiglas chamber (35 × 20 × 20 cm) that was placed on a shock grid made from stainless steel rods (Gass et al., 1998). The grid was connected to a shocker–scrambler unit delivering shocks of defined duration and intensity. For both contextual and cued conditioning, mice were placed into the Plexiglas chamber for 2 min before the onset of a discrete conditioned stimulus (2800 Hz tone; 85 dB) that lasted 30 sec. At the end of the tone, animals were subjected to the unconditioned stimulus (2 sec of continuous footshock at 0.8 mA). Animals were left in the conditioning chamber for another 30 sec and were then placed back into their home cages. Twenty-four hours after training, conditioning was assessed by measuring freezing, defined as a complete lack of movement besides respiration. For contextual conditioning, freezing was measured for 5 min in the same chamber in which the animals were trained. For the analysis of cued conditioning, animals

were placed in a novel context (triangular cage with nongrid floor and lemon smell). Two minutes later, the tone started for a period of 3 min during which freezing was assessed. Freezing was scored in 10 sec intervals, and the score was calculated in percentage of total observation time.

RESULTS

Generation of two different PAC1-deficient mouse lines

To disrupt *PAC1 in vivo*, we developed two different mutant mouse lines using the Cre/loxP recombination system (Gu et al., 1994). To inactivate all splice variants of *PAC1* known so far, we targeted exon 11 encoding the largest part of transmembrane domain IV of the receptor protein (Arimura, 1998). After homologous recombination in ES cells, we generated two different *PAC1* alleles (Fig. 1*a*). The *PAC1*$^{-}$ allele lacking exon 11 was injected into blastocysts to generate PAC1$^{-/-}$ mice with an ubiquitous inactivation of *PAC1*. In the *PAC1*^{loxP} allele, exon 11 was flanked by two *loxP* recognition sites (Fig. 1*a*) for Cre recombinase-mediated excision of the intervening DNA sequence. *PAC1*^{loxP} will therefore be inactivated in any cell expressing the recombinase. Mice homozygous for *PAC1*^{loxP} appear normal and expression of PAC1 mRNA is identical to that of wild-type mice (data not shown). For generation of mutant mice with a forebrain-specific inactivation of *PAC1* (*PAC1*^{loxP}/loxP-CaMKCre2, abbreviated PAC1^{CaMKCre2}), PAC1^{loxP} mice were bred with transgenic mice (CaMKCre2 mice) expressing the Cre recombinase under the control of the CaMKIIα promoter. In this transgenic CaMKCre2 line, Cre recombinase expression is restricted to the olfactory bulbs, cortical forebrain areas, and the hippocampus. Within the striatum very few scattered neurons express the Cre recombinase, whereas no expression is detected in the thalamus, the amygdala, the midbrain, the hindbrain, and the cerebellum (data not shown).

According to the expression pattern of the Cre recombinase, PAC1^{CaMKCre2} mice show an inactivation of *PAC1* in three brain areas, the olfactory bulbs, the cortical areas of the forebrain (data not shown), and the dentate gyrus (Fig. 1*f*). Conversely, PAC1$^{-/-}$ mice show an ubiquitous inactivation of *PAC1*. Wild-type transcripts of *PAC1* are completely absent (Fig. 1*b*,*e*). Instead, an alternatively spliced transcript reaching 8% of the wild-type RNA levels is detectable in PAC1$^{-/-}$ brains (Fig. 1*b*). Sequencing of this transcript reveals alternative splicing from exon 10–12, leading to a frame shift with subsequent stop codon (data not shown) and resulting in a truncated receptor molecule that because of the absence of the third intracellular loop cannot couple to G-proteins any longer. Interestingly, the other known PACAP receptors *VPAC1* and *VPAC2*, belonging to the class of PACAP type II receptors, are not upregulated in PAC1$^{-/-}$ mice (Fig. 1*c*).

At the age of weaning, PAC1^{CaMKCre2} mice are found at the expected Mendelian ratio ($n = 381$), whereas PAC1$^{-/-}$ mice are found at a frequency of 19% instead of 25% ($n = 589$). Both types of mutants are fertile, appear healthy, and are indistinguishable from their wild-type littermates. Histological analysis of organs from both mutant mouse lines does not reveal any pathological abnormalities (data not shown). Especially within the hippocampal formation neither neuronal proliferation nor differentiation defects nor mossy fiber abnormalities are observed (data not shown). A neurological examination including testing on a hot plate as well as testing of reflexes, motoric strength, and coordination (rotarod) does not reveal any deficits in sensory or motor abilities (data not shown).

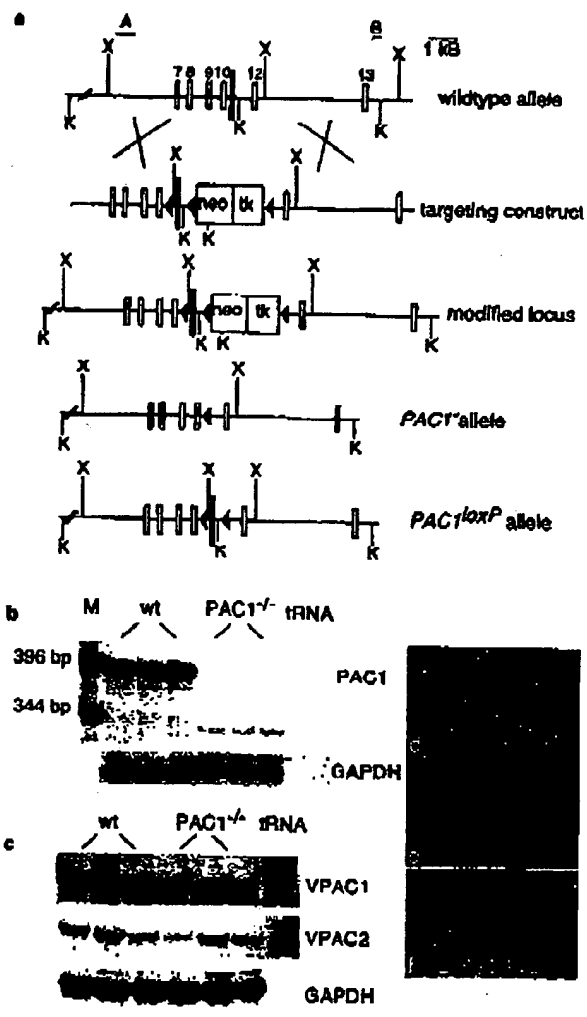

Figure 1. Generation of PAC1-deficient mice. *a*, Organization of *PAC1* encompassing exons 7–13. We flanked exon 11 (*black box*) with loxP sites in two steps. First, we generated the modified allele by homologous recombination in ES cells. Second, transient expression of Cre recombinase led to removal of the selection cassette, generating *PAC1*$^{-}$ and *PAC1*^{loxP} alleles. A scheme of the wild-type locus, the targeting vector, and the resulting alleles is depicted (*black triangles*, *loxP*; *K*, *KpnI*; *X*, *XbaI*; *A* and *B* represent probes outside of the homology arms used for Southern blot analysis of electroporated ES cells). *b*, *c*, RNase protection analysis of total brain RNA from wild-type (*wt*) and PAC1$^{-/-}$ mice. *b*, Although the 400 bp wild-type transcript is absent in PAC1$^{-/-}$ brains, a faint 340 bp fragment is detectable, representing an alternatively spliced transcript giving rise to a truncated receptor protein. *c*, PACAP type II receptors (VPAC1 and VPAC2) are not upregulated in PAC1$^{-/-}$ brains (*M*, 1 kb ladder). *d–f*, *In situ* hybridization of control, *PAC1*$^{-/-}$, and PAC1^{CaMKCre2} brains. In comparison with control (*d*), PAC1 mRNA is almost completely absent in the hippocampal region of PAC1^{CaMKCre2} brains (*f*) and also not detectable in PAC1$^{-/-}$ brains (*e*).

Impairment of mossy fiber LTP in PAC1-deficient mice

Because of the strong and restricted expression of PAC1 protein in hippocampal mossy fiber terminals (Otto et al., 1999), we studied first synaptic plasticity at the mossy fiber synapse

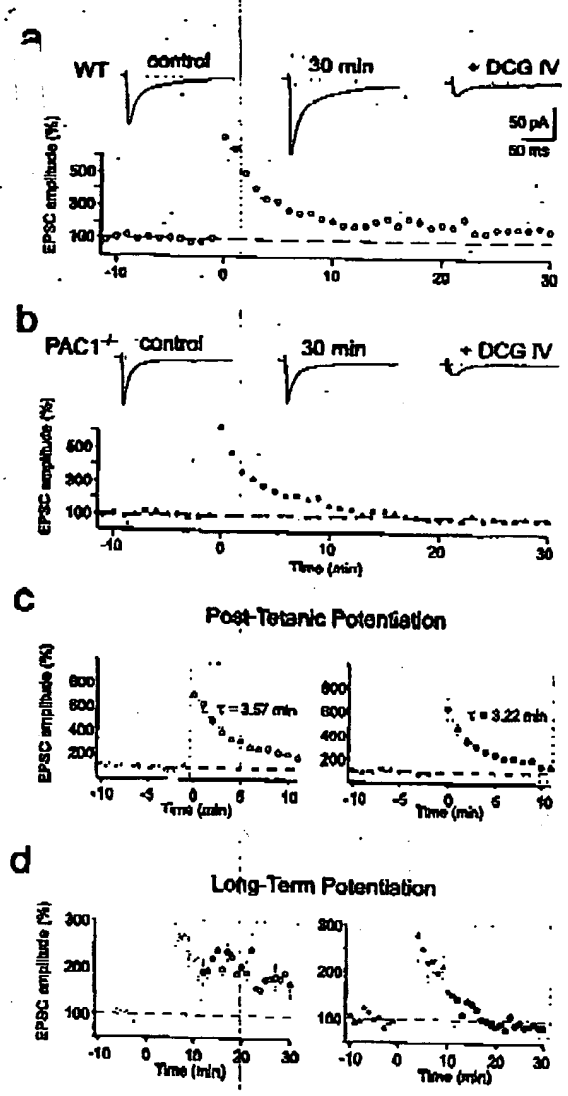

Figure 2. Mossy fiber LTP is impaired in PAC1$^{-/-}$ mice. *a*, *b*, LTP summary graphs in wild-type (*white circles*; mean ± SEM; 5 cells) and PAC1$^{-/-}$ (*black circles*; 7 cells) mice. *Insets above* show sample traces of EPSCs before (*control*), 30 min after tetanization (*30 min*), and after 1 μM DCG-IV bath application (*+ DCG IV*) in wild-type (*a*, *WT*) and PAC1$^{-/-}$ (*b*, *PAC1*$^{-/-}$) mice. LTP was induced by a stimulus train lasting for 5 sec at 25 Hz that was delivered at time 0. Each current trace is an average of 9–15 consecutive records. All recordings were done at room temperature (21–25°C). *c*, *d*, Different representation of the graphs shown in *a* and *b* to stress the similarity of PTP (*c*) and the difference in LTP (*d*) in wild-type and PAC1$^{-/-}$ mice, respectively. Note that the *y*-axes were scaled differently in *c* and *d*. The *two solid lines* in *c* represent exponential fits for the first 10 min of the decay phase of PTP yielding a time constant of τ = 3.57 min (*WT*, *left paired graph*) and τ = 3.22 min (*PAC1*$^{-/-}$, *right panel graph*). All recordings were done at room temperature (21–25°C).

(Zalutsky and Nicoll, 1990; Yeckel et al., 1999) in wild-type and PAC1-deficient mice. In wild-type animals, a train of high-frequency stimulation produced MF-LTP (Fig. 2*a*). Its characteristic features are the initial, strong PTP of the EPSC amplitude (mean EPSC amplitudes reached 710 ± 350% of control value; $n = 5$; mean ± SD) (Fig. 2*a*,*c*, *left panel*), followed by a sustained component of long-lasting potentiation (185 ± 57% of control value, measured at 25–30 min; $n = 5$) (Fig. 2*a*). This MF-LTP lasted for the entire duration of recording, typically 30 min of recording after the tetanus (Fig. 2*a*,*d*, *left panel*). By contrast, a similar conditioning stimulation applied to MFs of PAC1$^{-/-}$ mice, while evoking a similar PTP (630 ± 340% of control; $n = 7$) (Fig. 2*c*, *right panel*), produced in seven of seven cells no long-lasting potentiation (Fig. 2*b*,*d*, *right panel*). At ~15 min after conditioning, the EPSC amplitude returned to the control value and reached 90 ± 28% ($n = 7$) of the control amplitude after 25–30 min (Fig. 2*b*,*d*, *right panel*). These results indicate that PAC1 is selectively required for the sustained component of MF-LTP (Fig. 2*d*), but not for PTP (Fig. 2*c*). To ensure that the recorded EPSCs were predominantly caused by mossy fiber LTP, DCG-IV, an agonist of metabotropic glutamate receptors of the group 2/3 subtype (mGluR2/3), was applied to the bath solution (Yokoi et al., 1996; Castillo et al., 1997). DCG-IV (1 μM) reduced the amplitude of the EPSC by 60–90% (Fig. 2*a*,*b*), confirming that the recorded EPSCs were predominantly caused by mossy fiber synapses.

It is important to note that PPF (Salin et al., 1996), another form of short-term potentiation at these synapses, was also not affected (Fig. 3*c*) [PPF ratio was 209 ± 54% ($n = 5$) and 205 ± 67% ($n = 7$) in wild-type and mutant mice, respectively].

Although the evidence presently available points toward a rather selective presence of PAC1 at mossy fiber terminals (Otto et al., 1999), it seemed nevertheless interesting to test whether deficiency of the receptor interferes with LTP in hippocampal granule cells, the neurons from which mossy fibers originate. For this purpose, we performed whole-cell recordings from visually identified granule cells (Kellor et al., 1991) and stimulated perforant path fibers. Long-term potentiation at synapses formed between perforant path fibers and granule cells (PP-LTP) occurred in both wild-type (142 ± 27% of control, measured 40 min after conditioning; $n = 6$) and mutant mice (130 ± 29% of control; $n = 6$) (Fig. 3*a*,*b*). This intracellularly recorded LTP was very similar to that recorded extracellularly by other investigators (Lynch et al., 1985; Hansc and Gustafsson, 1992). The mean level of potentiation in PAC1$^{-/-}$ mice seemed to be somewhat smaller than in wild-type mice (Fig. 3*a*), however, the difference was not statistically significant (Student's *t* test; $p > 0.1$). Thus, taken together, the results of our cellular analyses clearly demonstrate that impairment of LTP in PAC1-deficient mice occurs predominantly at mossy fiber buttons, the only site at which PAC1 has been detected immunohistochemically in the hippocampus (Otto et al., 1999).

Associative but not declarative learning is impaired in PAC1-deficient mice

Because PAC1-deficient mice display a strong impairment of mossy fiber LTP, we investigated whether learning and memory is also impaired in these mouse mutants. We first analyzed mutants of both lines in two hippocampus-dependent tasks that model declarative learning and memory, the Morris water maze (Fig. 4*a*,*b*) and the social transmission of food preference (Fig. 4*c*). Neither PAC1$^{-/-}$ nor PAC1^{CaMKCre2} mice (data not shown) exhibit any deficits in these learning paradigms (Fig. 4*b*,*c*). During the acquisition phase, wild-type and mutant animals learn to search for the platform, as evidenced by the reduction of time needed to find the platform at the end of the training phase (Fig. 4*a*). During the probe trial of the Morris water maze, mutant and

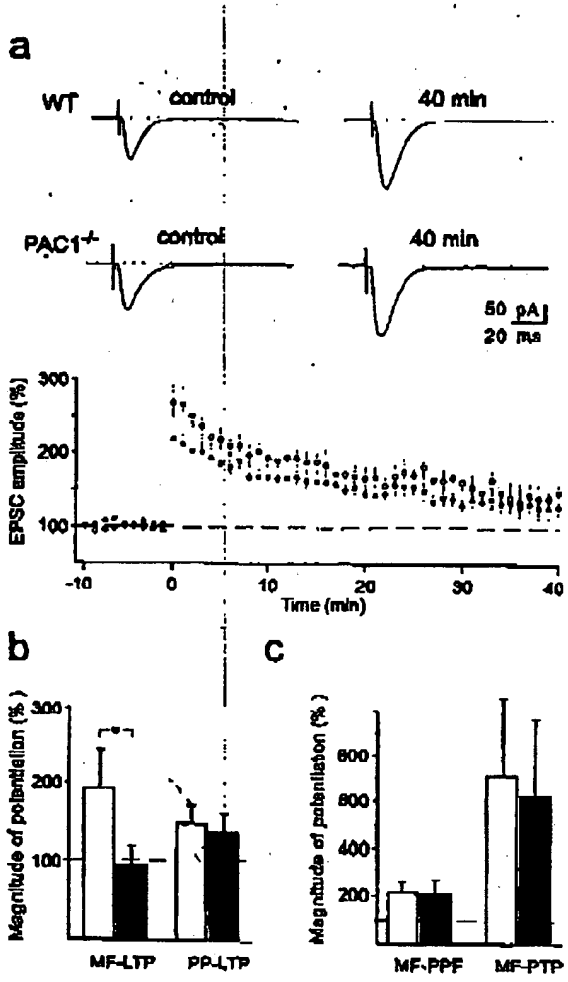

Figure 3. Preservation of LTP at the perforant path synaptic inputs to hippocampal granule cells in PAC1 $^{-/-}$ mice. *a*, LTP summary graph in wild-type (*white circles*; mean ± SEM; 6 cells) and PAC1 $^{-/-}$ (*black circles*; 6 cells) mice. *Inset* illustrates sample EPSC traces before (*control*) and 40 min after LTP induction (40 min) in wild-type (*WT*, *top traces*) and PAC1 $^{-/-}$ (*PAC1*$^{-/-}$, *bottom traces*) mice. Each current trace is an average of 9–15 consecutive records. LTP was induced by five 100 msec lasting stimulation trains at 100 Hz separated by 15 sec intervals, while the cell was current-clamped at −50 mV. Recordings were done at 30–32°C. *b*, Summary graph (mean ± SD) of the magnitude of LTP in wild-type (*white bars*) and PAC1 $^{-/-}$ (*black bars*) mice examined in mossy fiber to CA3 pyramidal cell synapses (*MF-LTP*, from data shown in Fig. 2*a*,*b*) and lateral perforant path to granule cell synapse (*PP-LTP*, from data shown in Fig. 3*a*). A significant change was observed only for MF-LTP ($^{*}p < 0.001$). MF-LTP was measured at room temperature (21–25°C), whereas PP-LTP was measured at 30–32°C (see Materials and Methods). *c*, Summary graph (mean ± SD) of the magnitude of paired-pulse facilitation (*MF-PPF*) and post-tetanic potentiation (*MF-PTP*) at mossy fiber to CA3 pyramidal cell synaptic inputs from wild-type (*white bars*; $n = 5$) and PAC1 $^{-/-}$ (*black bars*; $n = 7$) mice. There was no significant difference between wild-type and mutant mice. Recordings were done at room temperature (21–25°C).

wild-type animals searching for the platform spent significantly more time in the trained quadrant than in the other three quadrants, indicating that both groups have learned and remember the old platform position equally well (Fig. 4*b*). There are also no

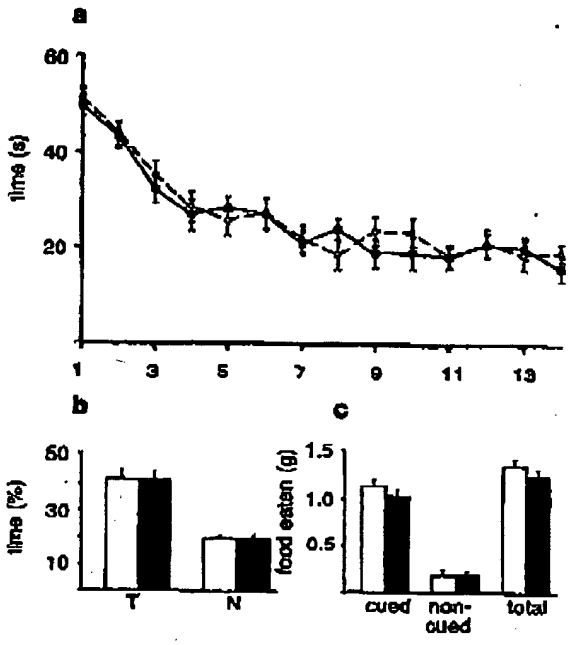

Figure 4. PAC1 $^{-/-}$ mice do not display any memory deficits in declarative learning tasks. *a*, Acquisition phase of the Morris water maze. The average values of two daily trials over a training period of 2 weeks are depicted. Wild-type ($n = 28$; *broken line*) and PAC1 $^{-/-}$ ($n = 28$; *solid line*) as well as PAC1 ^{CaMKCre2} mice (data not shown) learn the task equally well, as evidenced by the reduction of time needed to find the platform at the end of the training period. *b*, Probe trial of the Morris water maze. Wild types (*white bars*) and mutants (*black bars*) have learned and remember the old platform position equally well. In search of the platform, they spend significantly more time in the trained quadrant (*T*) than on average in the other three quadrants (*N*). *c*, Social transmission of food preference. PAC1 $^{-/-}$ as well as PAC1 ^{CaMKCre2} mice (data not shown) do not display any memory deficits in the social transmission of food preference. Mutants ($n = 28$; *black bars*) and wild types ($n = 28$; *white bars*) eat significantly more of the cued than of the non-cued food and thus remember exactly the food eaten by the demonstrator mouse 24 hr before.

deficits in the social transmission of food preference; mutants and wild-type animals eat significantly more of the cued than of the non-cued food, indicating that they remember exactly the food eaten by the demonstrator mouse 24 hr before (Fig. 4*c*).

Motivated by the finding that *Drosophila* carrying a mutation in the PACAP-related gene *amnesiac* display associative learning deficits (Quinn et al., 1979), we next analyzed the mice in a nondeclarative, associative learning paradigm, i.e., fear conditioning. For the interpretation of the results, it is noteworthy that in the conditioning chambers mutant mice of both strains showed comparable preshock locomotor activities to their wild-type littermates (PAC1 ^{CaMKCre2} line: mutants, 585 ± 34.6; wild types, 584 ± 42 activity counts; $p = 0.98$; PAC1 $^{-/-}$ line: mutants, 561 ± 25.7; wild types, 520 ± 33.3 activity counts; $p = 0.34$). PAC1 $^{-/-}$ as well as PAC1 ^{CaMKCre2} mice show a drastic reduction of the freezing response in the long-term test of contextual fear conditioning (Fig. 5), which is thought to be hippocampus- and amygdala-dependent (Kim and Fanselow, 1992; Phillips and LeDoux, 1992; Maren and Fanselow, 1996). After reexposure into the cage where conditioning had taken place 24 hr before, wild-

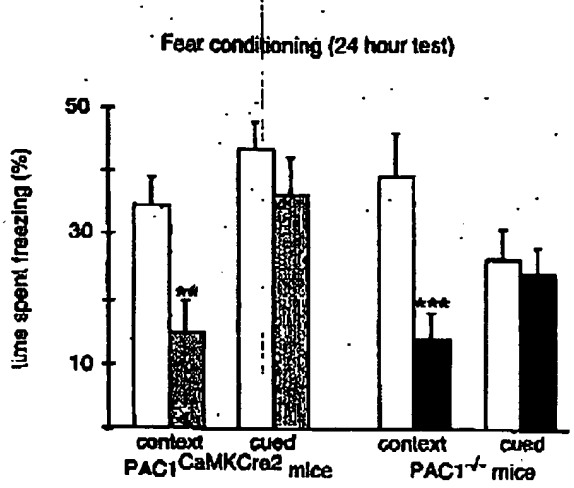

Figure 5. $PAC1^{-/-}$ and $PAC1^{CaMKCre2}$ mice show a selective deficit in hippocampus-dependent associative learning. $PAC1^{-/-}$ mice [$n = 14$ mutants (*black bars*), 14 wild types (*white bars*); $p < 0.005$] as well as $PAC1^{CaMKCre2}$ mice [$n = 12$ mutants (*gray bars*), 20 wild types (*white bars*); $p < 0.01$] exhibit a strongly reduced freezing response in contextual but not cued fear conditioning (24 hr test).

type animals remembered the contextual environment and showed a strong freezing response, whereas mutants of both lines started to explore the cage as if they had never seen it before. However, both mutant mouse lines did not show any deficits in the long-term test of cued fear conditioning (Fig. 5), a test that is thought to be amygdala-dependent (Kim and Fanselow, 1992; Philips and LeDoux, 1992; Maren and Fanselow, 1996). Mutants of both mouse lines showed in response to the tone a very similar freezing behavior as their wild-type littermates (Fig. 5). These findings clearly demonstrate a crucial role for PAC1-mediated signaling in associative, but not declarative, learning processes.

DISCUSSION

In this study, we investigated the potential role of PAC1-mediated signaling in synaptic plasticity as well as its impact on learning and memory. We used the Cre/loxP recombination system (Gu et al., 1994) to generate two different mutant mouse strains on the same genetic background. For the first time, we present evidence that PAC1 is involved in synaptic plasticity at the mossy fiber synapse and in associative learning. The generation of a conditional and a complete knock-out mouse line on the same genetic background allows direct comparison of both mouse lines and may circumvent developmental effects that often hamper analysis of conventional mouse knock-out models. In our conditional mouse line, PAC1 is inactivated postnatally in cortical forebrain areas and the hippocampus.

In parallel to our study, two different conventional PAC1-deficient mouse strains have been developed, but they have not been analyzed in learning paradigms (Hashimoto et al., 2000; Jamen et al., 2000).

A role of PAC1-mediated signaling for hippocampus-dependent associative learning and memory

As evidenced by the probe trial of the Morris water maze and the social transmission of food preference, both mutant mouse lines do not display any deficits in declarative learning tasks. Because hippocampal expression of *PAC1* is restricted to the mossy fiber synapse (Otto et al., 1999), the absence of spatial learning deficits (Morris water maze) and the absence of LTP impairment at the Schaffer collateral (Hashimoto et al., 2000) in the mutant mice is not surprising. In contrast to the Schaffer collateral pathway, the mossy fiber synapse seems to be less important for spatial learning (Chen and Tonegawa, 1997). Large parts of information are likely to be transmitted directly from the entorhinal cortex to pyramidal cells of CA3 and CA1, bypassing the mossy fiber synapse and not following the traditional trisynaptic circuit (Yeckel and Berger, 1990). The pivotal role of the Schaffer collateral for spatial learning is further evidenced by gene knock-out models of CaMKIIα (Silva et al., 1992), *fyn* (Grant et al., 1992), and PKCγ (Abeliovich et al., 1993), which all lead to an impairment of Schaffer collateral LTP and deficits in spatial learning.

Whereas declarative learning remains unaffected, both mutant mouse lines show a selective impairment of associative learning, i.e., contextual fear conditioning. This finding is very exciting because *Drosophila* harboring a mutation in the PACAP-related gene *amnesiac* display also associative learning deficits (Quinn et al., 1979). Therefore, the extreme evolutionary conservation of the neuropeptide PACAP and its type I receptor PAC1 may parallel their implication in a phylogenetically old learning paradigm, i.e., associative learning. Meanwhile, many components of the neuronal pathways involved in fear conditioning are known (Maren and Fanselow, 1996). The basolateral complex of the amygdala seems to be the putative locus for the association of the conditioned (tone, context) and unconditioned (footshock) stimulus. Sensory information is conveyed via two distinct inputs to the basolateral amygdala complex. Whereas auditory stimuli are processed to the amygdala via the medial geniculate nucleus of the thalamus, contextual stimuli reach the amygdala via the hippocampal formation. The basolateral complex of the amygdala projects to the central nucleus, which is connected with several brain areas involved in the generation of fear responses, such as the lateral hypothalamus (increase of blood pressure) or the periaqueductal gray (freezing response) (Maren and Fanselow, 1996). With regard to this pathway, lesions of the amygdala or the periaqueductal gray lead to an impairment of the freezing response in contextual as well as cued fear conditioning (Liebman et al., 1970; Campeau and Davis, 1995). Lesions of the hippocampus lead to impaired contextual but do not affect cued fear conditioning (Kim and Fanselow, 1992; Philips and LeDoux, 1992; Maren and Fanselow, 1996). The hippocampus is known to play within a critical time window a crucial role for the consolidation of contextual fear into long-term memory (Kim and Fanselow, 1992; Anagnostaras et al., 1999). Because mutants of both mouse lines display a dissociation between intact cued but impaired contextual fear conditioning, we conclude in accordance with the existing model of fear conditioning (Maren and Fanselow, 1996) that this phenotype reflects a hippocampus-dependent learning deficit. Importantly, an extensive neurological examination did not reveal any evidence for deficits of the sensory afferents necessary for processing contextual information. Furthermore, neither the Morris water maze task (vision) nor the social transmission of food preference (olfaction) revealed any deficits. Finally, because freezing in response to the tone was also not affected, the fear conditioning pathway in the amygdala and downstream of the amygdala must be intact (Maren and Fanselow, 1996).

Thus, we conclude that PAC1-mediated signaling in the hippocampus is required for contextual fear conditioning. In direct support of this view, we found that the brain regions with a

complete inactivation of *PAC1* in PAC1$^{-/-}$ as well as PAC1^{CaMKCre2} mice are the dentate gyrus and neocortical areas of the forebrain, but not the amygdala or the periaqueductal gray. In these latter regions *PAC1* is only inactivated in PAC1$^{-/-}$ but not PAC1^{CaMKCre2} mice. Because lesions of the neocortex do not impair contextual fear conditioning (Phillips and LeDoux, 1992; Chen et al., 1996), PAC1-mediated signaling in the hippocampus seems to play the critical role for the consolidation of contextual fear into long-term memory.

PAC1 is a novel determinant of synaptic plasticity at the mossy fiber synapse

The immunohistochemical data (Otto et al., 1999) and the electrophysiological results provide strong evidence that, within the hippocampus, the mossy fiber terminals represent the predominant site of PAC1-mediated signaling. At the mossy fiber synapse, LTP is distinctly different from LTP at all other hippocampal synapses. It is NMDA receptor-independent, and its induction requires an increase in the presynaptic calcium level (Nicoll and Malenka, 1995) and, under certain conditions, also postsynaptic calcium signaling (Yeckel et al., 1999). Although the molecular mechanism for LTP at the mossy fiber synapse is not known yet, there is strong evidence that the presynaptic calcium increase activates adenylate cyclases (Huang et al., 1994; Weisskopf et al., 1994). It has been hypothesized that activated adenylate cyclase type 1 (AC1) leads to an activation of PKA, which could cause an enhanced glutamate release by phosphorylation of proteins that influence the secretory machinery (Trudeau et al., 1996; Villacres et al., 1998). Rab3A is one of those candidates that contribute to PKA-mediated neurotransmitter release (Geppert et al., 1994). Within the hippocampus, PAC1 protein is exclusively expressed presynaptically in mossy fiber terminals (Otto et al., 1999). PAC1 can elevate intracellular calcium levels and activate PKA, two mechanisms, which were shown to determine long-term neuronal plasticity at the mossy fiber synapse (Huang et al., 1994; Weisskopf et al., 1994; Nicoll and Malenka, 1995). It is important to note that neither short-term synaptic plasticity at the mossy fiber synapse nor perforant path LTP were significantly impaired in the mutant mice. Similar results were previously obtained in Rab3A (Castillo et al., 1997) and AC1-deficient mice (Villacres et al., 1998). These findings are remarkable for two reasons: first, together with Rab3A knock-out mice (Castillo et al., 1997), PAC1-deficient mice are the first *in vivo* models that support the presynaptic locus of mossy fiber LTP expression. Second, the observed changes of neuronal plasticity at the mossy fiber synapse are identical with those seen in Rab3A (Castillo et al., 1997) and AC1-deficient mice (Villacres et al., 1998), which suggests that PAC1 may act in the same cascade upstream of AC1 and Rab3A activation. In conclusion, our findings identify a new mechanism through which PAC1 mediates neuronal signaling. PAC1-mediated signaling within the hippocampus seems to be largely restricted to mossy fiber terminals. Our results suggest that PAC1, through its involvement in a presynaptic form of hippocampal LTP, determines an associative form of hippocampal learning.

REFERENCES

Abelliovich A, Paylor R, Chen C, Kim JJ, Wehner JM, Tonegawa S (1993) PKCγ mutant mice exhibit mild deficits in spatial and contextual learning. Cell 75:1263–1271.

Anagnostaras SG, Maren S, Fanselow MS (1999) Temporally graded retrograde amnesia of contextual fear after hippocampal damage in rats: within-subjects examination. J Neurosci 19:1106–1114.

Arimura A (1998) Perspectives on pituitary adenylate cyclase activating polypeptide (PACAP) in the neuroendocrine, endocrine, and nervous systems. Jpn J Physiol 48:303–331.

Bliss TVP, Collingridge GL (1993) A synaptic model of memory: long-term potentiation in the hippocampus. Nature 361:31–39.

Campeau S, Davis M (1995) Involvement of the central nucleus and basolateral complex of the amygdala in fear conditioning measured with fear-potentiated startle in rats trained concurrently with auditory and visual conditioned stimuli. J Neurosci 15:2301–2311.

Castillo PE, Janz R, Südhof TC, Tzounopoulos T, Malenka RC, Nicoll RA (1997) Rab3A is essential for mossy fiber long-term potentiation in the hippocampus. Nature 388:590–593.

Chen C, Tonegawa S (1997) Molecular genetic analysis of synaptic plasticity, activity-dependent neural development, learning, and memory in the mammalian brain. Annu Rev Neurosci 20:157–184.

Chen C, Kim JJ, Thompson RF, Tonegawa S (1996) Hippocampal lesions impair contextual fear conditioning in two strains of mice. Behav Neurosci 110:1177–1180.

Christophe J (1993) Type I receptors for PACAP (a neuropeptide even more important than VIP?). Biochem Biophys Acta 1154:183–199.

Claiborne BJ, Xiang Z, Brown TH (1993) Hippocampal circuitry complicates analysis of long-term potentiation in mossy fiber synapses. Hippocampus 3:115–121.

Gass P, Wolfer DP, Balschun D, Rudolph D, Frey U, Lipp HP, Schütz G (1998) Deficits in memory tasks of mice with CREB mutations depend on gene dosage. Learn Mem 5:274–288.

Geppert M, Bolshakov VY, Siegelbaum SA, Takei K, De Camilli P, Hammer RE, Südhof TC (1994) The role of Rab3A in neurotransmitter release. Nature 369:493–497.

Grant SG, O'Dell TJ, Karl KA, Stein PL, Soriano P, Kandel ER (1992) Impaired long-term potentiation, spatial learning, and hippocampal development in *fyn* mutant mice. Science 258:1903–1910.

Gu H, Marth JD, Orban PC, Mossmann H, Rajewsky K (1994) Deletion of a DNA polymerase β gene segment in T cells using cell type-specific gene targeting. Science 265:103–106.

Hanse E, Gustafsson B (1992) Postsynaptic, but not presynaptic, activity controls the early time course of long-term potentiation in the dentate gyrus. J Neurosci 12:3226–3240.

Hashimoto H, Nogi H, Mori K, Ohishi H, Shigemoto R, Yamamoto K, Matsuda T, Mizuno N, Nagata S, Baba A (1996a) Distribution of the mRNA for a pituitary adenylate cyclase-activating polypeptide receptor in the rat brain: an *in situ* hybridization study. J Comp Neurol 371:567–577.

Hashimoto H, Yamamoto K, Hagigara N, Ogawa N, Nishino A, Aino H, Nogi H, Imamichi K, Matsuda T, Baba A (1996b) cDNA cloning of a mouse pituitary adenylate cyclase-activating polypeptide receptor. Biochim Biophys Acta 1281:129–133.

Hashimoto H, Shintani N, Nishino A, Okabe M, Ikawa M, Matsuyama S, Itoh K, Yamamoto K, Tomimoto S, Fujita T, Hagihara N, Mori W, Koyama Y, Matsuda T, Nagata S, Baba A (2000) Mice with markedly reduced PACAP (PAC1) receptor expression by targeted deletion of the signal peptide. J Neurochem 75:1810–1817.

Huang YY, Li XC, Kandel ER (1994) cAMP contributes to mossy fiber LTP by initiating both a covalently-mediated early phase and macromolecular synthesis-dependent late phase. Cell 79:69–79.

Inagaki N, Yoshida H, Mizuta M, Mizuno N, Fujii Y, Gonoi T, Miyazaki J, Seino S (1994) Cloning and functional characterization of a third pituitary adenylate cyclase-activating polypeptide receptor subtype expressed in insulin-secreting cells. Proc Natl Acad Sci USA 91:2679–2683.

Ishihara T, Shigemoto R, Mori K, Takahashi K, Nagata S (1992) Functional expression and tissue distribution of a novel receptor for vasoactive intestinal polypeptide. Neuron 8:811–819.

James F, Persson K, Bertrand G, Rodriguez-Henche N, Puech R, Bockaert J, Ahren B, Brabet P (2000) PAC1 receptor-deficient mice display impaired insulinotropic response to glucose and reduced glucose tolerance. J Clin Invest 105:1307–1315.

Johnston MC, Mc Cormack RJ, Delgado M, Martinez C, Ganea D (1996) Murine T-lymphocytes express vasoactive intestinal peptide receptor I (VIP-RI) mRNA. J Neuroimmunol 68:109–119.

Kaestner KH, Hiemisch H, Luckow B, Schütz G (1994) The *HNF-3* gene family of transcription factors in mice: gene structure, cDNA sequence and mRNA distribution. Genomics 20:377–385.

Kellendonk C, Tronche F, Casanova E, Anlag K, Opherk C, Schütz G (1999) Inducible site-specific recombination in the brain. J Mol Biol 285:175–182.

Keller BU, Konnerth A, Yaari Y (1991) Patch clamp analysis of excitatory synaptic currents in granule cells of rat hippocampus. J Physiol (Lond) 435:275–293.

Kim JJ, Fanselow MS (1992) Modality-specific retrograde amnesia of fear. Science 256:675–677.

Liebman JM, Mayer DJ, Liebeskind JC (1970) Mesencephalic central gray lesions and fear-motivated behaviour in rats. Brain Res 23:353–370.

Lutz EM, Sheward WJ, West KM, Morrow JA, Fink G, Harmar AJ (1993) The VIP_2 receptor: molecular characterization of a cDNA

encoding a novel receptor for vasoactive intestinal peptide. FEBS Lett 334:3–8.
Lynch MA, Errington ML, Bliss TV (1985) Long-term potentiation of synaptic transmission in the dentate gyrus: increased release of [^{14}C]glutamate without increase in receptor binding. Neurosci Lett 62:123–129.
Maren S, Fanselow SM (1996) The amygdala and fear conditioning: has the nut been cracked? Neuron 16:237–240.
Milner B, Squire LR, Kandel ER (1998) Cognitive neuroscience and the study of memory. Neuron 20:445–468.
Nicoll RA, Malenka RC (1995) Contrasting properties of two forms of long-term potentiation in the hippocampus. Nature 377:115–118.
Otto C, Zuschratter W, Gass P, Schütz G (1999) Presynaptic localization of the PACAP-type-I-receptor in hippocampal and cerebellar mossy fibers. Mol Brain Res 66:163–174.
Phillips RG, LeDoux JE (1992) Differential contribution of amygdala and hippocampus to contextual and cued fear conditioning. Behav Neurosci 106:274–285.
Quinn WG, Sziber PP, Booker R (1979) The *Drosophila* memory mutant amnesiac. Nature 277:212–214.
Salin PA, Scanziani M, Malenka RC, Nicoll RA (1996) Distinct short-term plasticity at two excitatory synapses in the hippocampus. Proc Natl Acad Sci USA 93:13304–13309.
Shivers BD, Gores TJ, Gottschall PE, Arimura A (1991) Two high affinity binding sites for pituitary adenylate cyclase activating polypeptide have different tissue distribution. Endocrinology 128:3055–3065.
Silva AJ, Paylor R, Wehner JM, Tonegawa S (1992) Impaired spatial learning in α-calcium-calmodulin kinase II mutant mice. Science 257:206–211.
Swanson LW, Teyler TJ, Thompson RF (1982) Hippocampal long-term potentiation: mechanisms and implications for memory. Neurosci Res Prog Bull 20:613–768.
Trudeau LE, Emery DG, Haydon PG (1996) Direct modulation of the secretory machinery underlies PKA-dependent synaptic facilitation in hippocampal neurons. Neuron 17:789–797.
Villacres EC, Wong ST, Chavkin C, Storm DR (1998) Type I adenylyl cyclase mutant mice have impaired mossy fiber long-term potentiation. J Neurosci 18:3186–3194.
Weisskopf MG, Castillo PE, Zalutsky RA, Nicoll RA (1994) Mediation of hippocampal mossy fiber long-term potentiation by cyclic AMP. Science 23:1878–1882.
Yeckel MF, Berger TW (1990) Feedforward excitation of the hippocampus by afferents from the entorhinal cortex: redefinition of the role of the trisynaptic pathway. Proc Natl Acad Sci USA 87:5832–5836.
Yeckel MF, Kapur A, Johnston D (1999) Multiple forms of LTP in hippocampal CA3 neurons use a common postsynaptic mechanism. Nat Neurosci 2:625–633.
Yokoi M, Kobayashi K, Manabe T, Takahashi T, Sakaguchi I, Katsuura G, Shigemoto R, Ohishi H, Nomura S, Nakamura K, Nakao K, Katsuki M, Nakanishi S (1996) Impairment of hippocampal mossy fiber LTD in mice lacking mGluR2. Science 273:645–647.
Zalutsky RA, Nicoll RA (1990) Comparison of two forms of long-term potentiation in single hippocampal neurons. Science 248:1619–1624.

ACADEMIC PRESS

Biochemical and Biophysical Research Communications 297 (2002) 427–432

BBRC

www.academicpress.com

Breakthroughs and Views

Higher brain functions of PACAP and a homologous *Drosophila* memory gene *amnesiac*: insights from knockouts and mutants

Hitoshi Hashimoto,[a] Norihito Shintani,[a] and Akemichi Baba[a,b,*]

[a] *Laboratory of Molecular Neuropharmacology, Graduate School of Pharmaceutical Sciences, Osaka University, 1-6 Yamadaoka, Suita, Osaka 565-0871, Japan*

[b] *Laboratory of Molecular Pharmacology, Graduate School of Medicine, Osaka University, Suita, Osaka 565-0871, Japan*

Received 12 August 2002

Abstract

Neuropeptides usually exert a long-lived modulatory effect on the small-molecule neurotransmitters with which they colocalize via regulation of the response times of second messenger systems. Pituitary adenylate cyclase-activating polypeptide (PACAP) functions as a neuromodulator and neurotransmitter and regulates a variety of physiological processes. PACAP is structurally highly conserved during evolution, implying its vital importance. In *Drosophila*, loss-of-function mutations in a PACAP-like neuropeptide gene, *amnesiac* (*amn*), affect both memory retention and ethanol sensitivity. The *amnesiac* gene is expressed in neurons innervating the mushroom body lobes, the olfactory associative learning center. Conditional genetic ablation of neurotransmitter release from these neurons mimics the *amnesiac* memory phenotypes, suggesting an acute role for *amnesiac* in memory. However, genetic rescue experiments also suggest developmental defects in *amnesiac* mutants, implying a role in neuronal development. There is a parallel between memory formation in *Drosophila* and mammals. PACAP-specific (PAC_1) receptor-deficient mice show a deficit in hippocampus-dependent associative learning and mossy fiber long-term potentiation (LTP). Meanwhile, PACAP-deficient mice display a high early mortality rate and additional CNS phenotypes including behavioral and psychological phenotypes (e.g., hyperlocomotion, intense novelty-seeking behavior, and explosive jumping). A functional comparison between PACAP and *amnesiac* underlines phylogenetically conserved functions across phyla and may provide insights into the possible mechanisms of action and evolution of this neuropeptidergic system.

PACAP and PACAP receptors in mammals

PACAP was first identified as a novel hypothalamic neuropeptide by Arimura's group in 1989, based on its ability to stimulate adenylate cyclase in cultured rat anterior pituitary cells [1]. PACAP exists in two amidated forms, PACAP38 and PACAP27, which share the same N-terminal 27 amino acids and are alternatively processed forms of a precursor, preproPACAP. PACAP27 has an amino acid sequence identity of 68% with vasoactive intestinal polypeptide (VIP) and of 37% with secretin, indicating that PACAP is a member of the VIP/glucagon/growth hormone-releasing hormone (GHRH)/secretin superfamily. This superfamily includes glucagon-like peptide-1 (GLP-1), GLP-2, glucose-dependent insulinotropic polypeptide (GIP), and peptide histidine methionine (PHM). PACAP is present not only in various areas of the central nervous system, including the hypothalamus and many other brain regions, but also in peripheral tissues such as the germ cells of the testes, different lobes of the pituitary gland, the adrenal medulla, pancreatic ganglia, and enteric nerves. It functions as a neuromodulator or neurotransmitter in the central and peripheral nervous systems (for reviews, see [2,3]).

Molecular cloning studies have shown that these diverse activities of PACAP are mediated by heptahelical G protein-linked receptors encoded by at least three different genes [4]. In 1991, Ishihara et al. [5] isolated a rat secretin receptor cDNA by expression cloning, and in 1992, they isolated a rat VIP ($VPAC_1$) receptor cDNA

* Corresponding author. Fax: +81-6-6879-8184.
E-mail address: baba@phs.osaka-u.ac.jp (A. Baba).

0006-291X/02/$ - see front matter
PII: S0006-291X(02)02144-7

by sequence homology to the secretin receptor [6]. The recombinant $VPAC_1$ receptor showed a similar high affinity for PACAP and VIP, and a low affinity for secretin. In 1993, in collaboration with Ishihara et al., we cloned a PACAP-preferring PAC_1 receptor, which binds PACAP with high affinity but binds VIP with a 1000-fold lower affinity [7]. Several other groups independently cloned the PAC_1 receptor [2–4]. Another VIP receptor subtype, $VPAC_2$, has also been cloned. The PAC_1 receptor is coupled to several transduction pathways, leading to the activation of adenylate cyclase, phospholipase C, mitogen-activated protein (MAP) kinases, and to calcium mobilization. In contrast, $VPAC_1$ and $VPAC_2$ are mainly coupled to the adenylate cyclase pathway. Although PACAP and VIP have no apparent homology with calcitonin and parathyroid hormone, PAC_1, VPAC, secretin, calcitonin, and parathyroid hormone/parathyroid hormone-related peptide (PTH/PTHrP) receptors are related to each other and constitute a subfamily of the G protein-coupled receptors [6,7].

Drosophila memory mutant *amnesiac*

Using the classical chemical mutagenesis with ethyl methane sulfonate, Quinn et al. [8] isolated the first *amnesiac* mutant in 1979 through a behavioral screening for memory mutants. *Amnesiac* flies show normal acquisition of an operant avoidance response but have impaired memory retention in the first few hours after training on associative learning tasks, in which flies receive an odor simultaneously with the negative reinforcement of electric shock (for reviews, see [9–12]). However, the isolation of the mutated gene proved difficult because the chemically mutated genes were not tagged. Transposon mutagenesis facilitates gene discovery by tagging the genes for cloning. Using a P-element mutagenesis and a simplified screening method, Feany and Quinn identified *amnesiac* cDNA and genomic DNA that encoded a predicted neuropeptide precursor [13]. Although the mature products of the *amnesiac* gene have yet to be identified, consensus cleavage sites suggest the existence of three potential peptides. Two of them have homology to the genes that encode vertebrate PACAP and GHRH (Figs. 1A and B). The first predicted peptide is homologous to GHRH [14] and the PACAP-related peptide (PRP) that is derived from preproPACAP [15] and shares some homology with GHRH. The second predicted *amnesiac* peptide is homologous to PACAP38 [1].

Mammalian PACAP38 has been shown to activate the potassium currents at the *Drosophila* neuromuscular

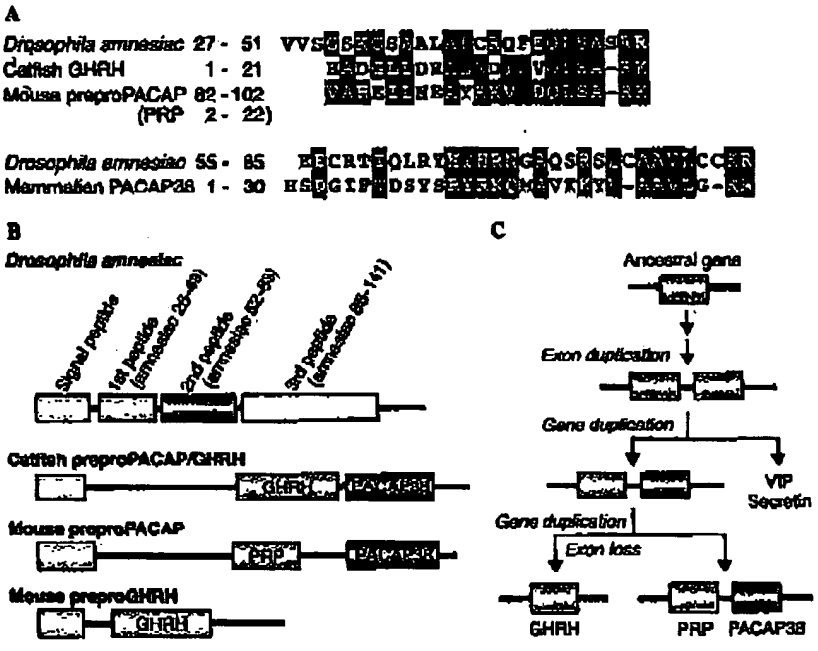

Fig. 1. Amino acid sequence alignment, precursor structures, and a hypothetical evolutionary scheme of the PACAP and GHRH gene family and *Drosophila amnesiac*. (A) Alignment of the amino acid sequences of the predicted *amnesiac* peptides and the mouse PACAP-related peptide (PRP [15]), the catfish GHRH [14], and the mammalian PACAP38 [1]. Identical amino acid residues are indicated in red and similar amino acid residues are indicated in orange (adapted from [13]). (B) Schematic representation of the predicted neuropeptide precursors encoded by *amnesiac*, the catfish preproPACAP/GHRH, the mouse preproPACAP, and the mouse preproGHRH. (C) A hypothetical evolutionary scheme of the PACAP and GHRH genes (adapted from [3]).

junction through activation of the cAMP and Ras/Raf signal transduction pathways [16]. In addition, PACAP38-like immunoreactivity has been found in the *Drosophila* nervous system. Thus, the putative *amnesiac* products are believed to act through adenylate cyclase to increase the cAMP levels [16,17].

The *Drosophila* learning mutants that have loss-of-function mutations in components of the cAMP cascade, *rutabaga* (adenylyl cyclase) and *DCO* (protein kinase A catalytic subunit), display increased sensitivity to ethanol. This is also the case for *amnesiac*, since Moore et al. [19] identified *cheapdate*, a mutant with enhanced sensitivity to ethanol [18], and revealed that *cheapdate* is allelic to *amnesiac*.

Phylogenetic evolution of PACAP and GHRH genes

The primary structure of the biologically active mature PACAP38 has been totally conserved between all mammalian species studied so far and is virtually unchanged between mammals, lower vertebrates, and protochordates (for reviews, see [2,3,20–22]). In contrast, the structure of GHRH is not well conserved, even between mammalian species. In mammals, PACAP and GHRH precursors are encoded by two distinct genes (Figs. 1B and C). The mammalian PACAP precursor contains both the 29-amino-acid PRP and PACAP38. Although the PRP shows some limited homology to PACAP27, it is more similar to GHRH. In contrast to mammals, in submammalian species including the chicken, frog, salmon, catfish, and possibly tunicates, PACAP and a GHRH-like peptide are encoded by the same gene (Fig. 1B). Thus, it appears that the GHRH/PACAP gene duplicated after the divergence of birds and mammals and exon loss gave rise to the mammalian GHRH gene, while mutation led to the formation of the mammalian PRP/PACAP gene. Fig. 1C shows a proposed model describing the evolution of these peptide precursor genes from a common ancestral gene [2,3,20–23]. It is presumed that, as in the case of the above-mentioned submammalian species, *Drosophila amnesiac* encodes both a PACAP-like peptide and a GHRH-like peptide.

Amnesiac localization, genetic ablation, and rescue experiments

The olfactory learning-related *Drosophila* proteins that have been localized to date are, in general, preferentially expressed in the mushroom bodies, which are key components of odor learning [10]. However, the amnesiac protein is not expressed in the mushroom bodies. Instead, it is quite specifically expressed in a pair of neurons called the dorsal paired medial (DPM) neurons that broadly innervate the mushroom body lobes [24]. The *shibire* gene encodes the fly homolog of dynamin, a GTPase that is essential for synaptic vesicle recycling. Conditional genetic ablation of the neurotransmitter release from DPM neurons by expression of a semidominant and temperature-sensitive *shibire* mutant [25] mimics the *amnesiac* memory phenotypes [24]. This result demonstrates an acute role for DPM neurons in memory storage and suggests that the *amnesiac* neuropeptide is actively involved in this process. However, genetic rescue of *amnesiac* gene expression throughout development restored memory function, but not if the rescue was only during the adult stage [24,26]. The latter result also suggests a developmental defect in *amnesiac* mutants and implies a role for the gene products in the development of DPM neurons [12].

On the contrary, the ethanol-sensitive phenotype is rescued by *amnesiac* gene expression only in adult flies [19], suggesting that memory formation and ethanol sensitivity have different spatio-temporal requirements for *amnesiac* [26].

Roles of PACAP in hippocampal synaptic plasticity and associative learning in mice

Memory in both vertebrates and invertebrates involves alteration in the efficiency of synaptic transmission, otherwise known as long-term potentiation (LTP) and long-term depression (LTD). In the rodent brain, three PACAP receptor subtypes, PAC_1, $VPAC_1$, and $VPAC_2$, have been identified in different regions, including the hippocampus [3,6,7,27]. Extracellular recording in hippocampal slice preparations has demonstrated that 0.05 nM PACAP38 induces long-lasting facilitation of the basal transmission of CA1 synapses. The PACAP effect is blocked by the muscarinic antagonist atropine and partially blocked by the NMDA antagonist APV, and therefore shares a common mechanism with LTP [28]. However, a high dose (1 μM) of PACAP38 induced a long-lasting depression of transmission at the CA1 synapses [28] while at the same time causing an enhancement of the perforant path-granule cell synapses in the dentate gyrus (Fig. 2 [29]). Recently, we have reported the generation of PAC_1 receptor-targeted mice, which show no impairment in LTP in the perforant path-dentate gyrus synapses [30]. Two different PAC_1 receptor-deficient mouse strains have recently been developed separately from our colony [31,32]. Otto et al. [31] reported that LTP is impaired in the mossy fiber-CA3 synapses, in agreement with immunohistochemical data showing that PAC_1 is exclusively expressed in mossy fiber terminals.

Motivated by the observation that the *amnesiac* flies display associative learning deficits, Otto et al. [31] analyzed possible alterations in the learning and memory

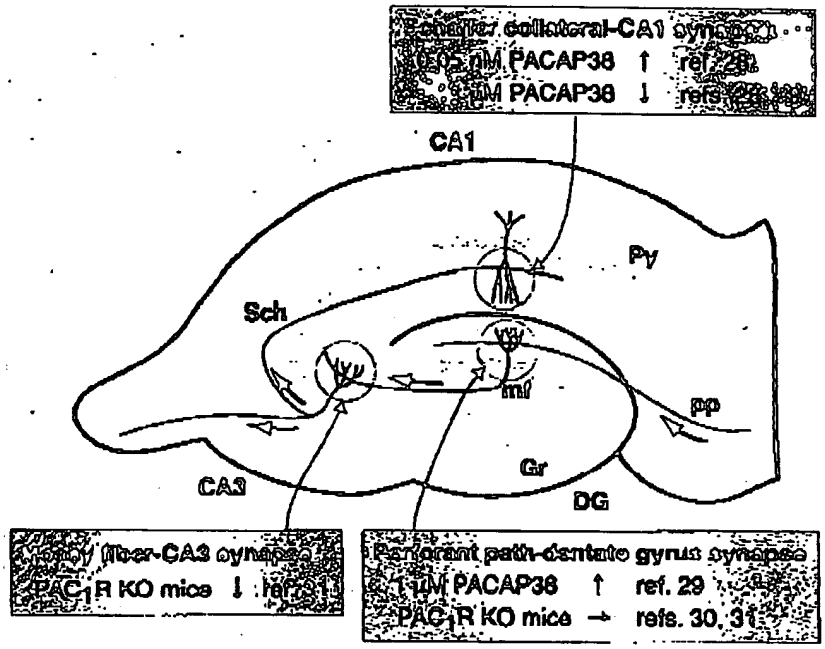

Fig. 2. The role of PACAP in hippocampal synaptic plasticity. pp, perforant path; DG, dentate gyrus; Gr, granular layer; mf, mossy fiber; Sch, Schaffer collateral; Py, pyramidal cell layer; CA, Ammon's horn (cornu ammonis); KO mice, knockout mice; ↑, induction of LTP; ↓, impairment of LTP or induction of LTD; →, no effect.

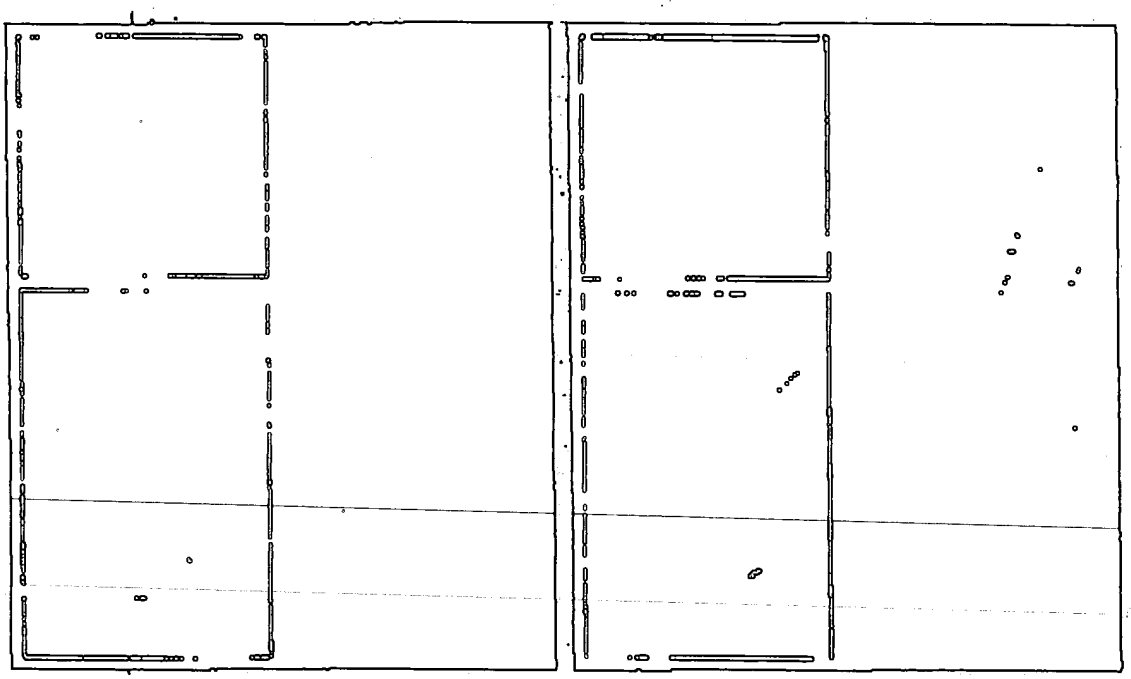

Fig. 3. Time-lapse photography showing hyperactivity and abnormal jumping behavior of PACAP-deficient mice (right) in comparison with wild-type control mice (left). Upper insets, examples of locomotor patterns during the last 10 min of a 60-min recording. Tracks of two representative mice in each group are shown. These hyperactive and jumping phenomena were originally reported in [33]. Reprinted with permission from [40].

features of their mutant mice using an associative fear learning paradigm. The mutant mice show a deficit in contextual fear conditioning, a hippocampus-dependent associative learning paradigm, although other hippocampus-dependent tasks such as the Morris water maze task are normal.

Behavioral and psychiatric phenotypes of PACAP-knockout mice

In another approach to understanding the in vivo function of PACAP-dependent signaling, we have generated mice deficient in PACAP ($PACAP^{-/-}$) [33]. The $PACAP^{-/-}$ mice are born in the expected Mendelian ratios, but have a high early mortality rate and approximately 50% of the $PACAP^{-/-}$ pups dies of unknown causes before weaning [33]. The surviving $PACAP^{-/-}$ females exhibit reduced fertility, which is partly due to reduced mating frequency, and show inadequate maternal behaviors [34]. In parallel to our study, two different PACAP-deficient mouse strains have been reported [35,36]. Gray et al. [36] reported dysfunction of lipid and carbohydrate metabolism in their PACAP knockout mice.

The surviving adult $PACAP^{-/-}$ mice display remarkable behavioral changes, including exhibition of hyperactive and explosive jumping behaviors in an open field, and increased exploratory behavior and less anxiety in the elevated plus-maze and two other behavioral tests (Fig. 3 [33]). These rather unexpected results may be ascribable to altered reinforcement as a result of perturbed monoamine neurotransmission. The serotonin metabolite 5-hydroxyindoleacetic acid (5-HIAA) is, in fact, decreased slightly in the $PACAP^{-/-}$ mice brain. Moreover, the aberrant behavior is ameliorated by the antipsychotic drug haloperidol [33].

Conclusions and outlook

Since it was demonstrated that the *amnesiac* mutants have mutations in a neuropeptide gene, the in vivo role of the mammalian homolog, PACAP, in higher brain functions has remained an open question [13,33]. Recent pharmacological studies and those in knockout mice now offer strong evidence, implicating PACAP-ergic neurons in the regulation of hippocampal synaptic plasticity, psychomotor activity, and emotional processes. It is currently unknown whether the mutant phenotypes resulted from developmental defects. Given the functional similarity between PACAP and *amnesiac*, it is possible that PACAP is required for proper brain function in both the developmental stages and the adult brain.

Resistance to ethanol has been correlated with alcoholism in humans [18]. Alcoholism and probably most types of drug addiction appear to share a common mechanism, namely the mesocorticolimbic reward system, which has been implicated in the control of novelty-induced locomotor activity and is a site of action for antipsychotic agents. In *Drosophila*, cocaine-induced behaviors show striking similarities to those induced in vertebrates [37]. In addition, cAMP signaling is involved in a number of plastic responses, including learning and memory, circadian rhythmicity, and responsiveness to cocaine and ethanol [38]. These observations imply a possible involvement of PACAP in the neurobiology of drug addiction.

Recently, *amnesiac* and its downstream target components, *pushover* (a Zn^{2+}-finger containing protein) and *NF1* (the *Drosophila* ortholog of the human gene responsible for type 1 neurofibromatosis), have been implicated in *Drosophila* perineurial glial growth [39]. Thus, causative genes and pathways identified in *Drosophila* may aid the future study of the human disease and vice versa. In addition, functional comparison between PACAP, the submammalian GHRH, and *amnesiac* underlines the phylogenetically conserved functions of this neuropeptide across phyla and may provide insights into the possible mechanisms of action and evolution of this peptidergic system.

Acknowledgements

Our research has been supported, in part, by a Grant-in-Aid for Scientific Research from the Ministry of Education, Culture, Sports, Science and Technology of Japan, and by grants from the New Energy and Industrial Technology Development Organization (NEDO) of Japan and Taisho Pharmaceutical Co. Ltd.

References

[1] A. Miyata, A. Arimura, R.R. Dahl, N. Minamino, A. Uehara, L. Jiang, M.D. Culler, D.H. Coy, Biochem. Biophys. Res. Commun. 164 (1989) 567–574.
[2] A. Arimura, Jpn. J. Physiol. 48 (1998) 301–331.
[3] D. Vaudry, B.J. Gonzalez, M. Basille, L. Yon, A. Fournier, H. Vaudry, Pharmacol. Rev. 52 (2000) 269–324.
[4] A.J. Harmar, A. Arimura, I. Gozes, L. Journot, M. Laburthe, J.R. Pisegna, S.R. Rawlings, P. Robberecht, S.I. Said, S.P. Sreedharan, S.A. Wank, J.A. Waschek, Pharmacol. Rev. 50 (1998) 265–270.
[5] T. Ishihara, S. Nakamura, Y. Kaziro, T. Takahashi, K. Takahashi, S. Nagata, EMBO J. 10 (1991) 1635–1641.
[6] T. Ishihara, R. Shigemoto, K. Mori, K. Takahashi, S. Nagata, Neuron 8 (1992) 811–819.
[7] H. Hashimoto, T. Ishihara, R. Shigemoto, K. Mori, S. Nagata, Neuron 11 (1993) 333–342.
[8] W.G. Quinn, P.P. Sziber, R. Booker, Nature 277 (1979) 212–214.
[9] R.L. Davis, Physiol. Rev. 76 (1996) 299–317.
[10] R.L. Davis, Neuron 30 (2001) 653–656.
[11] J. Dubnau, T. Tully, Annu. Rev. Neurosci. 21 (1998) 407–444.
[12] J. Dubnau, T. Tully, Curr. Biol. 11 (2001) R240–R243.

[13] M.B. Feany, W.G. Quinn, Science 268 (1995) 869–873.
[14] J.E. McRory, D.B. Parker, S. Ngamvongchon, N.M. Sherwood, Mol. Cell. Endocrinol. 108 (1995) 169–177.
[15] K. Yamamoto, H. Hashimoto, N. Hagihara, A. Nishino, T. Fujita, T. Matsuda, A. Baba, Gene 211 (1998) 63–69.
[16] Y. Zhong, Nature 375 (1995) 588–592.
[17] Y. Zhong, L.A. Pena, Neuron 14 (1995) 527–536.
[18] H.J. Bellen, Cell 93 (1998) 909–912.
[19] M.S. Moore, J. DeZazzo, A.Y. Luk, T. Tully, C.M. Singh, U. Heberlein, Cell 93 (1998) 997–1007.
[20] N.M. Sherwood, S.L. Krueckl, J.E. McRory, Endocr. Rev. 21 (2000) 619–670.
[21] M. Montero, L. Yon, S. Kikuyama, S. Dufour, H. Vaudry, J. Mol. Endocrinol. 25 (2000) 157–168.
[22] C.H. Hoyle, Regul. Pept. 73 (1998) 1–33.
[23] S. Ohkubo, C. Kimura, K. Oga, K. Okazaki, M. Hosoya, H. Onda, A. Miyata, A. Arimura, M. Fujino, DNA Cell Biol. 11 (1992) 21–30.
[24] S. Waddell, J.D. Armstrong, T. Kitamoto, K. Kaiser, W.G. Quinn, Cell 103 (2000) 805–813.
[25] T. Kitamoto, J. Neurobiol. 47 (2001) 81–92.
[26] J. DeZazzo, S. Xia, J. Christensen, K. Velinzon, T. Tully, J. Neurosci. 19 (1999) 8740–8746.
[27] H. Hashimoto, H. Nogi, K. Mori, H. Ohishi, R. Shigemoto, K. Yamamoto, T. Matsuda, N. Mizuno, S. Nagata, A. Baba, J. Comp. Neurol. 371 (1996) 567–577.
[28] M. Roberto, R. Scuri, M. Brunelli, Learn. Mem. 8 (2001) 265–271.
[29] T. Kondo, T. Tominaga, M. Ichikawa, T. Iijima, Neurosci. Lett. 221 (1997) 189–192.
[30] H. Hashimoto, N. Shintani, A. Nishino, M. Okabe, M. Ikawa, S. Matsuyama, K. Itoh, K. Yamamoto, S. Tomimoto, T. Fujita, N. Hagihara, W. Mori, Y. Koyama, T. Matsuda, S. Nagata, A. Baba, J. Neurochem. 75 (2000) 1810–1817.
[31] C. Otto, Y. Kovalchuk, D.P. Wolfer, P. Gass, M. Martin, W. Zuschratter, H.J. Grone, C. Kelleodonk, F. Tronche, R. Maldonado, H.P. Lipp, A. Konnerth, G. Schutz, J. Neurosci. 21 (2001) 5520–5527.
[32] F. Jamen, K. Persson, G. Bertrand, N. Rodriguez Henche, R. Puech, J. Bocksaert, B. Ahren, P. Brabet, J. Clin. Invest. 105 (2001) 1307–1315.
[33] H. Hashimoto, N. Shintani, K. Tanaka, W. Mori, M. Hirose, T. Matsuda, M. Sakaue, J. Miyazaki, H. Niwa, F. Tashiro, K. Yamamoto, K. Koga, S. Tomimoto, A. Kunugi, S. Suetake, A. Baba, Proc. Natl. Acad. Sci. USA 98 (2001) 13355–13360.
[34] N. Shintani, W. Mori, H. Hashimoto, M. Imai, K. Tanaka, S. Tomimoto, M. Hirose, C. Kawaguchi, A. Baba, Regul. Pept., 2002, in press.
[35] C. Hamelink, O. Tjurmina, R. Damadzic, W.S. Young, E. Weihe, H.W. Lee, L.E. Eiden, Proc. Natl. Acad. Sci. USA 99 (2002) 461–466.
[36] S.L. Gray, K.J. Cummings, F.R. Jirik, N.M. Sherwood, Mol. Endocrinol. 15 (2001) 1739–1747.
[37] C. McClung, J. Hirsh, Curr. Biol. 8 (1998) 109–112.
[38] S.K. Park, S.A. Sedore, C. Cronmiller, J. Hirsh, J. Biol. Chem. 275 (2000) 20588–20596.
[39] J. Yager, S. Richards, D.S. Hekmat Scafe, D.D. Hurd, V. Sundaresan, D.R. Caprette, W.M. Saxton, J.R. Carlson, M. Stern, Proc. Natl. Acad. Sci. USA 98 (2001) 10445–10450.
[40] A. Baba, Ann. Report Osaka Univ. 2001–2002, 2002, in press.

nature biotechnology

Production of knockout rats using ENU mutagenesis and a yeast-based screening assay

Yunhong Zan[1,2], Jill D Haag[1,2], Kai-Shun Chen[1], Laurie A Shepel[1], Don Wigington[1], Yu-Rong Wang[1], Rong Hu[1], Christine C Lopez-Guajardo[1], Heidi L Brose[1], Katherine I Porter[1], Rachel A Leonard[1], Andrew A Hitt[1], Stacy L Schommer[1], Anu F Elegbede[1] & Michael N Gould[1]

The rat is a widely used model in biomedical research and is often the preferred rodent model in many areas of physiological and pathobiological research. Although many genetic tools are available for the rat, methods to produce gene-disrupted knockout rats are greatly needed. In this study, we developed protocols for creating *N*-ethyl-*N*-nitrosourea (ENU)-induced germline mutations in several rat strains. F_1 preweanling pups from mutagenized Sprague Dawley (SD) male rats were then screened for functional mutations in *Brca1* and *Brca2* using a yeast gap-repair, *ADE2*-reporter truncation assay. We produced knockout rats for each of these two breast cancer suppressor genes.

The rat is an important murine model for studies in physiology, pathobiology, toxicology, neurobiology and a variety of other disciplines[1]. The rat is of value in these fields because it is larger than the mouse and because a plethora of organ-specific physiologic and disease models have been developed for it over the last century. The importance of the rat as a biological model has led to an intense effort to also establish it as a strong genetic model. A key genetic technology available for the mouse but not for the rat is the production of animals in which specified genes have been disrupted (knockout animals)[1]. This is due in part to the inability to produce functional rat embryonic stem cells. In addition, rats have not been generated to date by nuclear transfer (National Institutes of Health Meeting on Rat Model Priorities, May, 1999, http://www.nhlbi.nih.gov/resources/docs/ratmtgrp.htm). Here we report a method to produce knockout rats using an alternative approach.

The first step of our method consists of mutagenizing male rats with ENU. In mice, ENU is currently the mutagen of choice for the production of heritable altered phenotypes[2,3]. ENU was the most efficient mutagen tested[4] and was estimated to cause one functional mutation per 1,000 alleles tested (0.5–1.5 mutations per locus per progeny)[2,3]. It is important to stress the word 'functional' because the total number of mutations is much higher. Beier *et al.* calculated that theoretically there would be 10 actual sequence changes per 1,000 alleles, but that only 1 in 10 of these would result in a functional change leading to a phenotypic variant[5]. A main goal in this study was to develop a method that not only identifies F_1 rats with mutations in selected genes, but also prequalifies mutations that are likely to alter function, thus reducing wasted effort in downstream characterization of mutations that do not alter gene function. Thus, the second step of our approach involves yeast-based screening assays that select for various classes of functional mutations. These assays use gap-repair cloning to integrate either genomic DNA (gDNA) or cDNA of a selected gene between the yeast promoter ADH1 and the reporter gene *ADE2* to form a chimeric protein. If the DNA from a specific allele contains functional mutations that interfere with translation, then an active ADE2 chimeric protein is not produced, resulting in small, red yeast colonies instead of the large, white colonies found when screening wild-type DNA. We have combined ENU mutagenesis and yeast-based screening assays to generate two knockout rats for the breast cancer suppressor genes *Brca1* and *Brca2*.

RESULTS

Development of ENU mutagenesis protocols for the rat

Genome-wide mutagenesis protocols using ENU were established for three rat strains: inbred Wistar-Furth (WF), inbred Fischer 344 (F344) and outbred SD. Sexually mature 9-week-old male rats were given either a single intraperitoneal injection of ENU or a split dose with injections spaced a week apart. Fertility was determined at various times after ENU treatment (Table 1). The strains differed in their sensitivity to ENU-induced permanent sterility in a dose-dependent manner, with the WF strain being the most sensitive and the SD strain able to tolerate the highest doses. In all strains tested, ENU-treated male rats rarely recovered fertility after a period of complete sterility, unlike many strains of ENU-treated mice[6]. Average litter size was reduced in both the SD and F344 strains around weeks 7–9 after ENU treatment, the same time period in which we observed reduced fertility in the ENU-treated males. All fertile mutagenized male rats provided viable litters up to 1 year after ENU treatment; however, their lifespan was shortened, with many developing skin and kidney tumors and lymphomas at approximately 1 year of age. None of the doses listed in Table 1 were acutely toxic to the rat strains tested.

Mutagenized male rats were used to generate F_1 offspring, and phenotypically variant mutant pups were visually identified before weaning at 3–4 weeks of age. Abnormalities of the eyes, tail and growth were

[1]Department of Oncology, McArdle Laboratory for Cancer Research, 1400 University Avenue, University of Wisconsin-Madison, Madison, Wisconsin 53706, USA. [2]These authors contributed equally to this work. Correspondence should be addressed to M.N.G. (gould@oncology.wisc.edu).

Table 1 Effects of ENU treatment on male rat fertility and determination of heritable, phenotypic mutations of F_1 rats derived from ENU-treated male rats

Rat strain	ENU dose (mg/kg)	% male rats fertile[a]	No. phenotypic mutants observed[b]	Heritable	Non-heritable	Sterile	Unknown[c]
SD	75	100%	nd				
SD	100	80%	5/1068	0	1	0	4
SD	120	33%	2/347	0	1	0	1
SD	150	0%	nd				
SD	200	0%	nd				
SD	2×50	100%	4/524	1	2	0	1
SD	2×60	100%	74/4758	13	8	4	49
SD	2×75	20%	1/112	0	0	0	1
SD	2×100	0%	nd				
SD	0	100%	3/849	0	0	2	1
F344	75	100%	nd				
F344	100	67%	16/587	1	1	5	9
F344	120	0%	nd				
F344	2×50	60%	15/297	1	1	1	12
F344	2×60	40%	6/145	0	0	0	5
F344	2×75	0%	nd				
F344	2×100	0%	nd				
F344	0	100%	2/372	0	0	0	2
WF	25	30%	3/366	1	1	0	1
WF	35	33%	1/36	0	1	0	0
WF	50	25%	2/25	0	0	0	2
WF	75	0%	nd				
WF	100	0%	nd				
WF	2×15	17%	nd				
WF	2×25	17%	2/28	0	0	1	1
WF	2×50	0%	nd				
WF	2×75	0%	nd				
WF	0	100%	0/51	n/a	n/a	n/a	n/a

[a]ENU-treated male rats ($n = 3$–12) were paired with fertile female rats every 2 weeks from weeks 7–26 after ENU administration. Vaginal plugs were observed for all infertile breeding pairs. Fertility was based upon ability to produce a viable litter when bred with females of the same strain. [b]All F_1 pups from litters conceived at least 10 weeks after ENU treatment were visually examined for gross abnormalities in physical development or behavior at least twice before weaning at approximately 21 d of age. Details of the mutants are given in Supplementary Table 1 online. nd, not determined; n/a, not applicable. [c]Includes all phenotypic mutant F_1 rats that were not evaluated or that died before producing a litter.

those most commonly observed in the F_1 pups (see Supplementary Table 1 online). Using a split dose protocol of 2 × 60 mg ENU/kg body weight in SD male rats, a screen of visually apparent phenotypes revealed a rate of phenotypically detectable mutants of 1 in 64 F_1 rats (Table 1 and Supplementary Table 1 online). A subset of the phenotypic mutant F_1 rats was tested for inheritance. Approximately one-half of those that produced viable litters showed heritability of the trait (Tables 1 and 2 and Fig. 1).

Development of a yeast-based assay for mutation screening

We chose to use the outbred SD rat for the mutation-screening studies owing to its tolerance of ENU treatment, to the variety of ENU-induced, heritable phenotypic mutants identified and to its large litter sizes. We used a split dose of ENU (2 × 60 mg/kg) to mutagenize male SD rats. These rats were then bred to wild-type female SD rats to produce F_1 pups that were screened for mutant alleles of *Brca1* and *Brca2*.

Two related truncation assays[7,8] were developed to screen the *Brca1* and *Brca2* genes of these F_1 pups for functional mutations that could interfere with protein translation (Fig. 2). The first assay uses gDNA as a starting macromolecule, whereas the second assay begins with total RNA that is reverse-transcribed to cDNA. In both assays, PCR is used to amplify fragments of the gDNA exon or the cDNA targeted for knockout (Fig. 2). The gap-repair vectors are customized for each targeted fragment by cloning in small 5′ and 3′ sequences from the fragment of interest. For *Brca1*, three vectors were generated, and the third vector (used for the cDNA assay) is shown in Fig. 2. For *Brca2*, three vectors were also generated and the second is shown in Fig. 2. The 5′ and 3′ end sequences from each fragment were cloned in tandem and separated by a unique *Sma*I restriction enzyme site, which allows the plasmid to be linearized. The linearized vector is then transformed together with unpurified PCR product of the gene-specific fragment into competent yeast (*S. cerevisiae*, yIG397 strain) cells. Following transformation, the gene-specific fragment is cloned *in vivo* into the gap-repair vector by homologous recombination. Once incorporated into the vector, the gene fragment is then located behind the yeast promoter *ADH1* and in front of the reporter gene *ADE2*, with which it jointly codes for a functional chimeric protein. This yeast strain lacks ADE2 function that can be restored by this chimeric protein. Yeast cells that produce chimeric ADE2 protein grow efficiently and form large white colonies when plated on selective medium. In the absence

Table 2 ENU-induced heritable phenotypes

Line	Strain	F_1 founder sex	Initial ENU dose (mg/kg)	Observed phenotype	Confirmed in multiple litters
9	F344	Female	100	No left eye	Yes
18	SD	Female	2 × 60	Crooked tail and slit eyes	Yes
19	SD	Male	2 × 50	Growth on tail[a]	Yes
28	SD	Female	2 × 60	Red ring eyes[a]	Yes
29	SD	Female	2 × 60	Oblong face	Yes
32	SD	Female	2 × 60	Slit eyes[a]	Yes
38	SD	Male	2 × 60	Curved tail	Yes
42	SD	Female	2 × 60	Bald spots	Yes
44	F344	Female	2 × 50	Hooklike tail[a]	Yes
54	SD	Female	2 × 60	Scaly skin	Yes
56	WF	Female	25	Head tilt	Yes
60	SD	Female	2 × 60	Scaly skin	Yes
61	SD	Male	2 × 60	Swollen feet	Yes
63	SD	Male	2 × 60	Additional digits on hind feet[a]	Yes
64	SD	Male	2 × 60	Additional digits on hind feet	Yes
68	SD	Male	2 × 60	Kinked tail	No[b]
71	SD	Male	2 × 60	Curly hair and whiskers[a]	No[b]

[a]Observed altered phenotypes are shown in Figure 1. [b]Only one litter has been produced to date; however, breeding of founder rat is ongoing.

of functional chimeric protein the yeast cells grow poorly and form small red colonies. Thus, for *Brca1* and *Brca2*, if the DNA donor F_1 pup is wild type for the incorporated gene fragment, the assay yields large white colonies. If, however, the donor rat DNA contains a functional mutation in one allele of *Brca1* or *Brca2* in the assayed fragment, the translation of a functional hybrid ADE2 protein is prevented and small red colonies are produced. In this assay, a functional mutation for *Brca1* and *Brca2* in a rat will be heterozygous; therefore, approximately half the colonies will be red and half white after accounting for a background rate of red colonies.

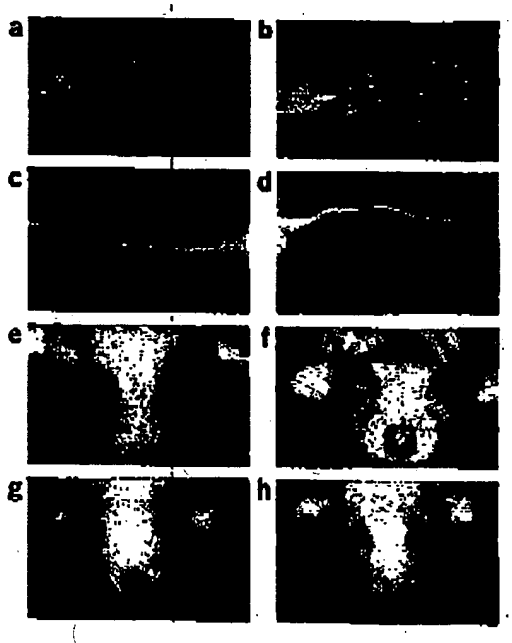

Figure 1 Heritable phenotypic mutant rats. Male rats were given ENU and then bred to produce F_1 pups that were observed for visible altered phenotypes. Details of these derivations are listed in Table 2. The phenotypic mutants and control rats shown include: (a) line 63 rat with multiple digits on hind foot; (b) control rat hind foot; (c) line 19 rat with growths on tail; (d) line 44 rat with hook-like tail; (e) line 28 rat with red ring eyes; (f) line 32 rat with slit eyes; (g) line 71 rat with curly hair and whiskers, no eye abnormality; (h) control rat.

Establishment of a *Brca2* knockout rat line

We looked for disruption of the *Brca2* gene with a gDNA assay, focusing on exon 11 (the largest exon, representing roughly half of the cDNA) (Fig. 2). This large exon was divided into three regions of ~1,700 base pairs (bp) each, and the second and third fragments were used for screening. Primer sequences for each fragment are given in Supplementary Table 2 online. We screened gDNA from 788 preweanling F_1 rat pups before finding a mutated *Brca2* allele using the second-fragment vector (Fig. 2). The knockout rat was the only one identified with this *Brca2* mutation out of 296 F_1 offspring screened from this specific mutagenized father, indicating that this mutation was not a preexisting germline mutation in this SD father. Similarly, the female parent produced over 40 offspring, including 10 littermates of the knockout rat, none of which carried the *Brca2* mutation. The *Brca2* knockout rat was detected in our gDNA assay by a yeast plate that had approximately 45% red colonies and 55% white colonies (Fig. 3a, right dish). The average background of red colonies was very low (Fig. 3a, left dish) for this gDNA assay (0.5% ± 0.6%, $n = 10$). Next, individual red and white yeast colonies were sequenced. A nonsense transversion mutation was detected at nucleotide T4254 of the *Brca2* cDNA that converted TAT (tyrosine) to TAA (stop codon) at Tyr1359 (Fig. 3a, lower panel, upper and center sequences). A/T→T/A transversion mutations are the most common mutation type (44%) found in mice bearing ENU-induced, phenotypically detectable germline mutations[4,5]. Genomic DNA from the founder rat 3983 was sequenced and found to contain the identical mutation as detected in the yeast red colonies (Fig. 3a, lower panel, lower sequence).

In conjunction with the gDNA assay, we used the cDNA yeast assay with the same *Brca2* fragment 2 vector to screen N_2 pups resulting from the breeding of the *Brca2* knockout founder male rat 3983 to SD females. Both methods identified the same 9 out of 14 pups from the first litter of rats carrying this *Brca2* mutation, and these results were confirmed by the direct sequencing of gDNA from each N_2 pup. This verified the utility of the yeast assay starting from either gDNA or RNA. This cDNA assay had a background of 15.3% ± 2.0% ($n = 20$) for wild-type pups and 48.5% ± 2.1% ($n = 36$) red colonies for knockout pups. Sequencing *Brca2* fragment 2 DNA of 60 red colonies from the cDNA assay of the knockout pups confirmed this background frequency, in that 17% (10/60) of the sequenced clone fragments lacked the specific stop codon mutation. Interestingly, the

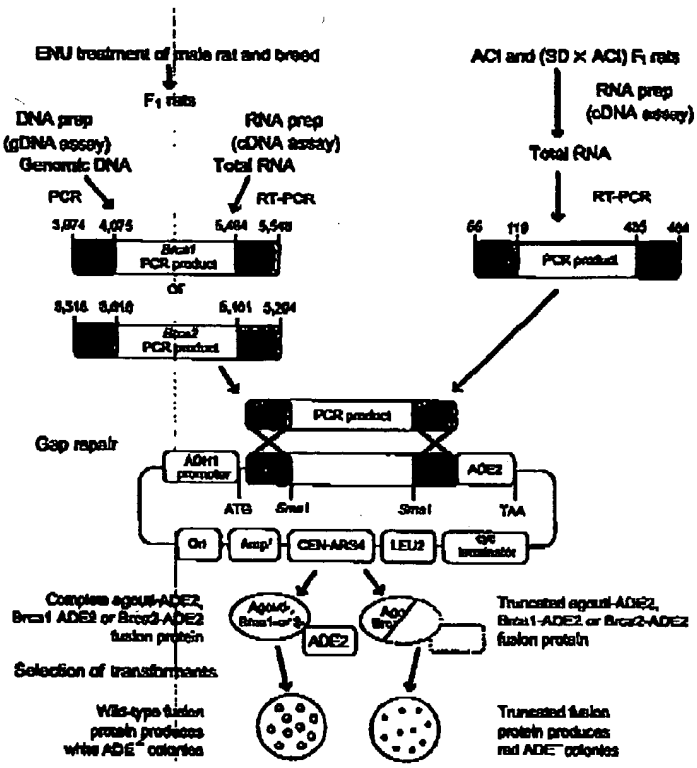

Figure 2 *Brca1*, *Brca2* and *agouti* yeast cDNA/gDNA truncation assays. For *Brca1* and *Brca2* assays, male rats are treated with ENU and bred to produce F_1 pups. DNA and RNA are isolated from tail clips of one-week-old F_1 rats for *Brca1* and *Brca2*. For the *A (agouti)* assays, a small piece of ventral skin from ACI or (SD × ACI) F_1 rats is excised and used for RNA isolation. Total RNA is reverse-transcribed and both the resultant cDNA (*Brca1* or *A*) and isolated gDNA (*Brca2*) are amplified using PCR for selected DNA regions. The gap repair vectors are customized for each targeted fragment. The 5′ and 3′ sequences for the *Brca1* vector are derived from nucleotides 3974–4075 and 5464–5548 of the *Brca1* cDNA (GenBank no. AF036760), respectively. The 5′ and 3′ sequences for the *Brca2* vector are derived from nucleotides 3518–3618 and 6101–6204 of the *Brca2* cDNA (GenBank no. U89653, mRNA), respectively. The *Brca1* and *Brca2* vectors shown are those that ultimately led to the identification of the knockouts. A single gap vector was constructed using the 5′ and 3′ sequences derived from nucleotides 55–119 and 435–484 of the *A* mRNA sequence (GenBank no. AB045587), respectively. Following transformation, the gene-specific fragment is cloned *in vivo* into the gap-repair vector by homologous recombination. The wild-type gene fragment codes for a functional fusion protein with the *ADE2* gene of the vector and forms large white colonies when plated. A truncated gene fragment will not form a functional protein and the colonies will be small and red.

background rate for the cDNA assay was over an order of magnitude higher than the gDNA assay, suggesting that most of the background in the cDNA assay comes from DNA replication errors in the reverse transcription reaction.

N_2 pups produced from founder 3989 included 35 heterozygous knockouts out of 64 pups, demonstrating the mendelian inheritance of this knockout gene. *Brca2* heterozygous N_2 male and female rats were bred to produce *Brca2* homozygous knockout pups. The ratio of *Brca2* homozygous knockout rats to *Brca2* heterozygous rats to wild-type rats was approximately 1:2:1. Body weight data were collected for all N_2F_2 pups starting at weaning. The results illustrate a clear phenotype of growth inhibition of male and female *Brca2* homozygous knockout rats (Fig. 3b). These rats are sterile and reduced in size but otherwise healthy. Histopathological analysis of gonads from the *Brca2* homozygous rats shows severe atrophy that is not observed in the *Brca2* heterozygous and wild-type rat gonads (Supplementary Fig. 1 online).

Production of a *Brca1* mutant rat line

Customized gap-repair vectors for screening *Brca1* (Fig. 2) consisted of two gDNA vectors targeting exon 11 (the largest exon, target fragments 1 and 2) and one cDNA vector targeting *Brca1* from the 3′ end of exon 11 to the end of the open reading frame (ORF) (fragment 3). Primer sequences for the three fragments are given in Supplementary Table 2 online. After screening 1,965 pups, we identified a *Brca1* mutation in founder rat 5385 using the cDNA assay (Fig. 2). This rat was the only one with this mutation identified in 270 offspring from the same mutagenized SD father and in more than 40 offspring, including 14 littermates, from the SD wild-type mother. The background rate of red colony formation in this assay was 12.2% ± 3.3% (n = 1,485) for wild-type DNA compared to 44.3% in the identified mutant. Haploid DNA from red yeast colonies was sequenced, revealing a complete loss of *Brca1* exon 22 (74 bp) (Fig. 4). We sequenced introns 21 and 22 in search of a splicing mutation to explain the loss of this exon. A T→C mutation was identified within the splicing branch site of intron 21 (TGGTGAT to TGGCGAT) (Fig. 4d,e). A T/A→G/C transition mutation is the second most common type (38%) of ENU-induced mutations[2,3]. The mutation in the branch site of intron 21 caused the splice donor site to skip over exon 22 and find a branch site in intron 22. This led to splicing out of the 74-bp exon 22 and also caused a frameshift downstream from exon 21, exposing a stop codon at the exon 23–24 border (Supplementary Fig. 2 online). Recently, the female founder 5385 has produced two *Brca1* heterozygous rats out of eight pups, demonstrating germline transmission of this mutation.

Nonsense-mediated decay

An anticipated problem using RNA as a starting material for this assay is the potential destruction by cell surveillance mechanisms, such as nonsense-mediated decay (NMD)[9–11], of mRNA transcribed from the mutant allele. We quantified the extent of NMD of the mutated *Brca2* mRNA by comparing the yield of red colonies in the knockout rat samples minus background in the wild-type samples using the cDNA assay (48.5–15.3%) versus the yield of red colonies in the knockouts minus background using the gDNA assay (44.8–0.5%). The same gDNA *Brca2* fragment 2 gap vector was used for both the cDNA and gDNA assays. From these results, NMD is calculated to occur at an approximate rate of [1 – (33/44)] or 25%.

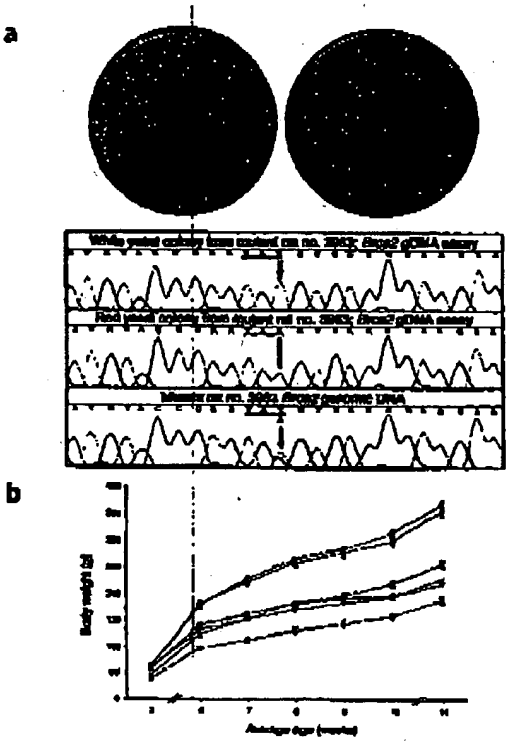

Figure 3 Identification of a *Brca2* knockout rat. (a) Screening for a *Brca2* knockout rat. Yeast cells transformed with gap vector and a PCR product enriched for *Brca2* fragment 2 (nucleotides 3518–5204) were plated on selective medium. When gDNA obtained from a rat (SD) with two wild-type alleles was assayed, the resultant plate contained mostly large white colonies (left dish). In contrast, when the DNA is from a rat in which one allele of *Brca2* was functionally mutated, the resultant colonies were an almost equal mixture of red and white colonies (right dish). Red and white colonies from the plate on the right were picked and used to obtain *Brca2* fragment 2 DNA sequence. The sequence from white yeast colonies (lower panel, upper, representative of four colonies tested) is that of wild-type rat *Brca2*, whereas the sequence from red colonies (lower panel, center, representative of eight colonies tested) has a transversion mutation at T4254 (indicated by the arrow) of the cDNA (TAT (tyrosine) → TAA (stop)). Genomic DNA from the heterozygous knockout rat no. 3983 contains both T and A at nucleotide 4254 as seen in the lower sequence (represents two independent tests). The sequences shown in the lower panel span nucleotides 4242–4266 of the rat *Brca2* cDNA. (b) *Brca2* knockout body weight phenotype. Male (solid orange lines) and female (dashed blue lines) *Brca2* homozygous (Δ), heterozygous (○) knockout rats and wild-type littermates (□) were weighed through their current age of 14 weeks (error bars are ± s.d.).

Because this level of NMD was modest, we challenged our cDNA-based assay using a rat *A* (also known as *agouti*) locus model in which ~85% of the mutant RNA is subject to NMD[11]. Agouti rat strains such as the ACI rat carry two copies of the wild-type locus, whereas nonagouti rats such as SD carry two identical mutant alleles, each with two truncating mutations in the *A* gene. We designed a yeast gap vector for this gene that allowed the entire ORF to be cloned *in vivo* in yeast (Fig. 2). We found that our cDNA assay could routinely detect the *A* mutation in (SD × ACI) F_1 pups, which had 12.4% ± 1.8% ($n = 52$) red colonies, whereas the wild-type ACI group had a background of 4.4% ± 1.6% ($n = 40$) red colonies ($P < 0.0001$, unpaired *t*-test). NMD was estimated to remove approximately 80% of the RNA coded from the mutated *A* allele of the F_1 pup, which corresponds well with the above-referenced northern analysis[11]. Note also that the lower background rate of 4.4% red colony formation for the *A* cDNA assay (500 bp) as compared to that of the *Brca1* (12.2%, 1.6 kb) and *Brca2* (15.3%, 1.7 kb) cDNA assays demonstrates that background is proportional to the size of the gene or gene fragment being screened. A second estimate of background was obtained by sequencing for the *A* mutation in individual red colonies from a yeast assay of the (SD × ACI) F_1 pups. Of 61 red colonies evaluated, 5 had random mutations, giving a background of 8%, statistically distinguishable from the F_1 value of 12.4% ± 1.8% red colonies ($P < 0.0001$, one-sample *t*-test).

DISCUSSION

We have established methods to produce knockout rats and have identified knockouts for *Brca1* and *Brca2*. Our technology combines protocols for efficient rat germline mutagenesis by ENU and a yeast-based method to economically (~$18,000 for a 90% chance of success) and rapidly screen preweanling F_1 rat pups from mutagenized fathers for functional mutations in selected genes using yeast truncation assays. The first identified rat gene to be knocked out, *Brca2*$^{6ch0-4254}$, was bred to homozygosity and has a phenotype that includes general growth inhibition and gonadal atrophy in both sexes. Interestingly, *Brca2* homozygous knockout mice with similar mutations in exon 11 have shown either embryonic lethality or embryonic survival with premature death[12–14]. We have not yet begun phenotypic evaluation of the *Brca1* knockout rat line.

Our ENU assay for the rat provides a phenotype-driven, ENU-induced mutation screening for a second murine species. The outbred SD rat tolerated the highest single and split dose of ENU. This and its ability to produce large litters led us to choose it for our genotype-based mutation screening. The inbred F344 strain tolerated higher doses than the very ENU-sensitive WF strain. It will be important in the future to evaluate additional inbred lines for their reproductive tolerance of ENU, as inbred rats provide a more homogenous genome than the more complex outbred rat strains, especially if evaluation of preexisting germline mutations is required. However, with either an inbred or outbred strain, it is important to backcross the knockout founder to either the isologous strain or another of a desired genetic background to eliminate other ENU-induced germline mutations. Switching genetic backgrounds may be more efficient in that it allows the use of speed congenic protocols. Furthermore, to eliminate the possible confounding effects of very closely linked mutations, one can screen for additional alleles of each knockout using this yeast-based technology and evaluate them phenotypically.

Our yeast-based truncation screening assays have advantages and disadvantages that suggest which one should be used to target specific genes. The gDNA assay is most efficient if the selected gene has at least one exon larger than ~400–500 bp. In contrast, the cDNA assay is independent of exon size and can easily incorporate up to ~2,500 bp per vector. However, the background rate of red colony formation is over an order of magnitude lower in the gDNA assay, making it easier to identify mutant rats through red colony formation on the yeast plates. These truncation assays allow screening only for mutations that compromise protein translation, such as nonsense mutations and out-of-frame frameshift deletions or insertions. The *Brca1* knockout rat was identified using a cDNA yeast truncation assay in the 3′ region of the *Brca1* gene that consists of a series of very small exons. None of the

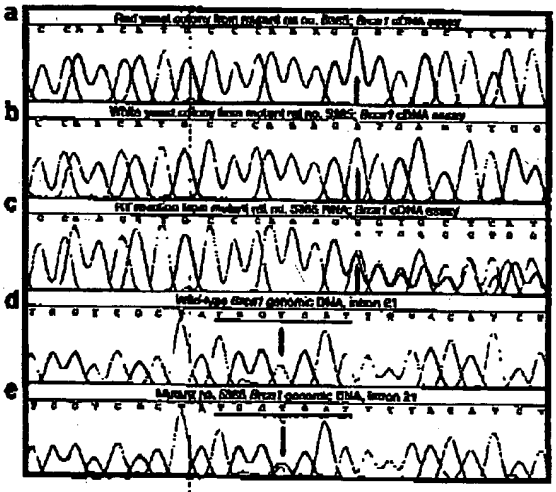

Figure 4 Screening for a *Brca1* knockout rat. Yeast cells were transformed with linearized gap vector and a PCR product enriched for *Brca1* fragment 3 (nucleotides 3974–5548). A plate with 44.3% red colonies (as compared to an average 15.8% red colony background from all other plates, $n = 89$) identified a potential knockout rat, no. 5385. (a) Sequence of haploid DNA from a yeast red colony (representative of eight colonies tested) in which exon 22 (74 bp) is deleted. (b) The sequence of haploid DNA from a wild-type white colony (representative of two colonies tested). The arrow in panel a indicates the first nucleotide (5359) of exon 23, whereas the arrow in panel b indicates the first nucleotide (5285) of exon 22. (c) This difference is highlighted by sequencing a mixture of cDNA from both rat alleles (+/−) from a reverse transcription reaction of total tail RNA (representative of two independent tests). In panels a, b and c, the sequence before the arrow is the 3′ end of exon 21. (d) Results of sequencing gDNA from a wild-type SD rat over a region of intron 21 that contains the splicing branch site (underlined). (e) The same sequence from the heterozygous *Brca1* mutant founder rat no. 5385, which includes a T→C mutation (indicated by the arrow) within the splicing branch site. Sequences in d and e span nucleotides 36–12 upstream of exon 22, with the mutation at nucleotide 24 upstream of exon 22. The mutant sequence is shown in its translated form in Supplementary Figure 2 online.

exons covered would have been good targets for the gDNA truncation assay because of their small size. In addition, this intronic mutation would not have been found using other screening methods, such as sequencing, heteroduplex analysis or denaturing high-performance liquid chromatography, because these assays are used to screen only the exons from gDNA.

The major drawbacks of the cDNA assay are that the gene-specific RNA may not be produced in an easily collectible tissue and mutant RNA may be lost to a great extent by NMD. In these studies, we demonstrate the ability of a cDNA yeast-based screening assay to detect the *A* mutant allele despite a high level of NMD in this model, and thus show the general ability of a yeast-based screening assay to detect mutants in spite of extensive NMD. NMD can be minimized by pretreating collected cells, such as white blood cells, with a protein synthesis inhibitor before RNA collection. This approach has been successful for the yeast gap-repair p53 assay[15,16] and may be extrapolated to *in vivo* studies by the administration of a protein synthesis inhibitor to rat pups before tissue collection. We have had preliminary success in inhibiting NMD using the protein synthesis inhibitor emetine. The problem of a gene-specific RNA not being produced in tail tissue may be reduced by extending the range of biopsy tissues collected from viable rats (for example, white blood cells, liver and skin). In the future, sperm from F_1 male rats of mutagenized fathers could be cryopreserved[17], and a wide variety of organ-specific RNAs could also be collected and stored, along with DNA from spleens or other tissue from the same male rats. DNAs or RNAs from a large number of rats could thus be screened and the appropriate frozen sperm used to recover mutant rats. Sperm cryopreservation has been established for many mouse strains and crosses[18] and has allowed the recovery of a mutant mouse[19].

In summary, the technologies presented here provide the means for producing gene-selected knockout lines for the rat. The generation of unique rat models should extend our knowledge of the genetics underlying human diseases and aid in the development of novel drugs to prevent and treat these diseases.

METHODS

Rat ENU mutagenesis protocol. The University of Wisconsin-Madison Animal Care and Use Committee has approved all experimental animal procedures described in these studies. We administered a single or split dose of ENU by intraperitoneal injection to male rats from Harlan at 9 weeks of age; for a split dose, at 9 and 10 weeks of age. One gram of ENU (Sigma) was dissolved in 10 ml of 95% (vol/vol) ethanol and then diluted with 90 ml of phosphate citrate buffer (0.2 M Na_2HPO_4, 0.1 M citric acid, pH 5.0) before injection. We paired mutagenized males with females of the same strain for consecutive 2- to 3-week periods, beginning 3–6 weeks after the first ENU treatment. We observed female rats for vaginal plugs, gross pregnancy, date of birth and size of litters. For our *Brca1* and *Brca2* mutation screening experiments, we used SD male rats given a split dose of ENU, 2 × 60 mg/kg body weight.

We collected tail clips from the F_1 pups at 1 week of age for macromolecule isolation. We also visually checked all F_1 pups for gross abnormalities in physical development at least twice before weaning at 21–28 d of age. A subset of the F_1 phenotypic mutant rats identified was bred to same-strain rats to determine inheritance of the phenotypic mutation. Several of the rat lines with heritable mutant phenotypes are currently being maintained and backcrossed to eliminate residual ENU-induced genetic changes not associated with the phenotypic mutations.

All breedings to produce ACI and (SD × ACI) F_1 pups were performed at our facility. At 5–7 d of age, pups were killed and ventral skin was collected for the *A* yeast assay.

Vector construction. The gap vector pLSRP53 containing the p53 cDNA[15,20] was digested with *HindIII* and *EagI* to remove the entire p53 coding sequence. A 44-bp linker that contains sequence encoding the first 11 amino acids of rat p53 was inserted at the *HindIII* and *EagI* sites to produce vector pLSR846 with the *EagI* site converted to a unique *NotI* site. The full length *ADE2* gene was amplified by PCR from yeast strain yIG397 (ref. 15) DNA and integrated into the pLSK846 plasmid at the *NotI* site to generate vector pLSK870. A unique *NotI* site was retained at the 5′ end of the *ADE2* gene. This *NotI* site was used to drop in *Brca1*, *Brca2* or *A* sequence cassettes. Each *Brca1*, *Brca2* or *A* cassette contained two fused ~100 bp fragments, corresponding to the 5′ and 3′ ends of a ~1.6 kb *Brca1* fragment, a ~1.7 kb *Brca2* fragment or the ~500 bp *A* ORF, joined by a unique *SmaI* site. The half-site sequences of the *Brca1*, *Brca2* or *A* cassettes were designed to be in frame with the p53 leader and *ADE2* sequences (Fig. 2). Vectors were linearized before yeast transformation by digestion with *SmaI* (20 U/μl) and then purified using a QIAquick PCR purification kit (Qiagen, Inc.).

DNA/RNA extraction. To isolate DNA, small sections of tails were digested overnight at 55 °C in 500 μl of genomic lysis buffer consisting of 20 mM Tris-HCl, pH 8.0, 150 mM NaCl, 100 mM EDTA and 1% (wt/vol) SDS. Two hundred μl of Protein Precipitation Solution (Gentra Systems) was added to the lysate solution. DNA in the clear supernatant was precipitated with isopropanol, washed and resuspended in water. Total RNA was isolated from tail or skin sections that were placed in RNAzol B solution (Tel-Test) and homogenized (Polytron PT10-35, Kinematica). The samples were then extracted with

chloroform, precipitated with isopropanol and washed with ethanol. Pellets were resuspended in 30 µl RNA suspension solution (Ambion) for *Brca1* and *Brca2*, and in 60 µl for *A*.

Reverse transcription and PCR. All primers used are listed in Supplementary Table 2 online. cDNA was synthesized for *Brca1* or *Brca2* from 1–2.5 µg rat tail total RNA at 42 °C for 2 h with 200 U of SuperScript II (Invitrogen). *A* cDNA was synthesized from 1–5 µg of skin total RNA in a 1 h reaction. The 20 µl reaction consisted of 1× reverse transcription buffer (Invitrogen), 0.5× RNA secure reagent (Ambion), 10 mM DTT, 1.25 mM dNTP mix and 0.33 µg *Brca1*-, *Brca2*-, or *A*-specific primers. PCR was performed on 1.0 µl of the cDNA product or ~0.1 µg of gDNA with 1 U of Herculase (Stratagene) in 20 µl reactions containing 1× Herculase buffer, 0.2 mM dNTP mix and 0.05 µg primers for *Brca1* and *Brca2*. Reaction conditions for *Brca1* and *Brca2* fragments were 95 °C for 2 min, followed by 35 cycles consisting of 1 min at 92 °C, 45 s at 60 °C, and 4 min at 72 °C, followed by 7 min at 72 °C. For the *A* gene PCR, 0.5 U of Failsafe enzyme (Epicentre Technologies) was used with Failsafe buffer J (which contains dNTPs) and 0.1 µg primers. The cycling conditions for *A* were similar to above except that the annealing temperature was 55 °C and the 72 °C extension step was only 1 min. PCR quality and product quantity were estimated by electrophoresis in a 1.2% (wt/vol) agarose gel.

Yeast transformation and sequencing. yIG397 (ref. 15) yeast was cultured overnight at 30 °C in YPD medium supplemented with adenine (200 µg/ml) to an OD_{600} of 0.9. The cells were washed and resuspended in a volume of LiOAc/TE solution (0.1 M lithium acetate, 10 mM Tris-HCl, pH 8.0, 1 mM EDTA) equivalent to the volume of the cell pellet. For each transformation, 30 µl of yeast suspension was mixed with 10 ng of linearized gap vector, 25 µg of salmon sperm carrier DNA, 150 µl of LiOAc/TE/PEG solution (0.1 M lithium acetate, 10 mM Tris-HCl, pH 8.0, 1 mM EDTA, 40% (wt/vol) PEG) and 2–5 µl unpurified *Brca1*, *Brca2*, or *A* PCR product (total volume ~185 µl). The mixture was incubated for 30 min at 30 °C, then heat-shocked for 15 min at 42 °C. Transformants were then plated on synthetic minimal medium lacking leucine and supplemented with low adenine (5 µg/ml) and incubated for 3 d at 30 °C. An automated colony counter (ProtoCOL, Microbiology International) was used to determine the number of red and white colonies on each plate for the cDNA assays, and the percentage of red colonies per sample was recorded. The background rate of red colonies was determined by averaging the percentage of red colonies from all plates not containing a knockout. gDNA assay yeast plates were generally inspected only visually. The signal-to-noise ratio for the gDNA assay was large (>50:1), whereas that for the cDNA assay was smaller (~3:1). Thus, a criterion for the cDNA assays was set to follow up on samples for which the red colony percentage was at least 2 s.d. above the mean. This conservative criterion was designed to avoid false negatives and the average resulted in two false positives per gene assay for 90 rats screened. Most false positives were eliminated upon repeating the yeast assay using the original RNA sample.

For sequencing, red and white colonies were picked directly into PCR mix, amplified and purified to remove primers and nucleotides. Four microliters of each reaction was then used in a 20 µl cycle-sequencing reaction using BigDye (Applied Biosystems Inc.) chemistry.

Note: Supplementary information is available on the Nature Biotechnology website.

ACKNOWLEDGMENTS

We thank Amy Mosey for discussions and suggestions during the course of this work; R. Iggo, M. Tada, and T. Moriuchi for providing the pLSRP53 plasmid and the yIG397 yeast strain used in this paper; Henry Prior for analysis of the histology sections; and Dinelli M. Monson and Millicent A. Shultz for technical assistance. This work has been supported by grants from the US National Institutes of Health (CA28954 and CA77494).

COMPETING INTERESTS STATEMENT

The authors declare that they have no competing financial interests.

Received 24 September 2002; accepted 13 March 2003
Published online 28 May 2003; doi:10.1038/nbt830

1. Jacob, H.J. & Kwitek, A.E. Rat genetics: attaching physiology and pharmacology to the genome. *Nat. Rev. Genet.* 3, 33–42 (2002).
2. Justice, M.J., Noveroske, J.K., Weber, J.S., Zheng, B. & Bradley, A. Mouse ENU mutagenesis. *Hum. Mol. Genet.* 8, 1955–1963 (1999).
3. Noveroske, J.K., Weber, J.S. & Justice, M.J. The mutagenic action of *N*-ethyl-*N*-nitrosourea in the mouse. *Mamm. Genome* 11, 478–483 (2000).
4. Russell, W.L. *et al.* Specific-locus test shows ethylnitrosourea to be the most potent mutagen in the mouse. *Proc. Natl. Acad. Sci. USA* 76, 5918–5922 (1979).
5. Geier, D.R. Sequence-based analysis of mutagenized mice. *Mamm. Genome* 11, 594–597 (2000).
6. Justice, M.J. *et al.* Effects of ENU dosage on mouse strains. *Mamm. Genome* 11, 484–488 (2000).
7. Ishioka, C. *et al.* Screening patients for heterozygous p53 mutations using a functional assay in yeast. *Nat. Genet.* 5, 124–129 (1993).
8. Kataoka, A. *et al.* Development of a yeast stop codon assay readily and generally applicable to human genes. *Am. J. Pathol.* 159, 1239–1245 (2001).
9. Culbertson, M.R. RNA surveillance. Unforeseen consequences for gene expression, inherited genetic disorders and cancer. *Trends Genet.* 15, 74–80 (1999).
10. Frischmeyer, P.A. & Dietz, H.C. Nonsense-mediated mRNA decay in health and disease. *Hum. Mol. Genet.* 8, 1893–1900 (1999).
11. Kuramoto, T., Nomoto, T., Sugimura, T. & Ushijima, T. Cloning of the rat agouti gene and identification of the rat nonagouti mutation. *Mamm. Genome* 12, 469–471 (2001).
12. Suzuki, A. *et al.* *Brca2* is required for embryonic cellular proliferation in the mouse. *Genes Dev.* 11, 1242–1252 (1997).
13. Connor, F. *et al.* Tumorigenesis and a DNA repair defect in mice with a truncating *Brca2* mutation. *Nat. Genet.* 17, 423–430 (1997).
14. Friedman, L.S. *et al.* Thymic lymphomas in mice with a truncating mutation in *Brca2*. *Cancer Res.* 58, 1338–1343 (1998).
15. Flaman, J.-M. *et al.* A simple p53 functional assay for screening cell lines, blood, and tumors. *Proc. Natl. Acad. Sci. USA* 92, 3963–3967 (1995).
16. Andreutti-Zaugg, C., Scott, R.J. & Iggo, R. Inhibition of nonsense-mediated messenger RNA decay in clinical samples facilitates detection of human MSH2 mutations with an *in vivo* fusion protein assay and conventional techniques. *Cancer Res.* 57, 3288–3293 (1997).
17. Natsuyama, E. *et al.* Generation of live rat offspring by intrauterine insemination with epididymal spermatozoa cryopreserved at −196 °C. *Reproduction* 122, 463–467 (2001).
18. Nakagata, N. Cryopreservation of mouse spermatozoa. *Mamm. Genome* 11, 572–576 (2000).
19. Coghill, E.L. *et al.* A gene-driven approach to the identification of ENU mutants in the mouse. *Nat. Genet.* 30, 255–256 (2002).
20. Yamamoto, K. *et al.* A functional and quantitative mutational analysis of p53 mutations in yeast indicates strand biases and different rates of mutations in DMBA- and BBN-induced tumors in rats. *Int. J. Cancer* 83, 700–705 (1999).